COPPER CANYON GOLD SKARN-A REVIEW

Geochemistry of the Gold Skarn Environment at Copper Canyon, Battle Mountain Mining District, Nevada - An Update

Boris B. Kotlyar, Ted G. Theodore and Donald A. Singer
U.S.G.S., Menlo Park, CA

Ken Moss and Arthur M. Campo
Battle Mountain Gold Co., Battle Mountain, NV

Modified from Kotlyar, B.B., Theodore, T.G., Singer, D.A., Moss, Ken, Campo, A.M., and Johnson, S.D., 1998, Geochemistry of the gold skarn environment at Copper Canyon, Nevada, in Lentz, D.R., ed., Mineralized intrusion-related skarn systems, Mineralogical Association of Canada Short Course Series, v. 26, p. 415–443.

Reprinted with permission from: Geological Society of Nevada, Fall 1999 Field Trip Guidebook, Special Publication No. 31, Geology and Gold Mineralization of the Buffalo Valley Area, Northwestern Battle Mountain Trend

Edited by Hans Rasmussen, White Knight Gold (US) Inc., 2005 for this publication.

INTRODUCTION

Historically, the Battle Mountain Mining District has been one of the largest producers of intrusion-related Au in north-central Nevada (**Fig. 1**), yielding approximately 3.5 million oz Au since 1978, when production shifted from base and precious metals to only precious metals. Geochemical data for the Fortitude Au skarn (the largest producer in the mining district at 2 million oz Au), for nine other relatively recently discovered nearby Au–Ag orebodies, and for mineralized drill core, along with production data from small polymetallic veins, reveal striking district- and deposit-scale metal zones around a 38 to 40 Ma skarnrelated porphyry Cu system at Copper Canyon (**Fig. 2**). Metal zoning is especially well developed at Copper Canyon. A Cu–Au–Ag zone in the central part of the porphyry center is mantled by a Au–Ag zone, which is, in turn, surrounded by a Pb–Zn–Ag zone (**Fig. 3**; Roberts and Arnold 1965; Theodore *et al.,* 1986; Myers 1994). Depth of oxidation is quite shallow in the area, which makes it ideally suited for studies involving primary elemental dispersion haloes in the third dimension. The Au–Ag zone at Copper Canyon subsequently was determined to host the Fortitude gold skarn, which was discovered during the winter of 1980–1981 (Wotruba *et al.,* 1986; Doebrich *et al.,* 1996). The Fortitude deposit also is mantled by elevated abundances of Hg which form a prominent hook-shaped pattern of anomalies around the northern part of the deposit (Kotlyar *et al.,* 1995).

The spatial zonation of metals around Au skarns has not been documented thoroughly in the North American literature (*cf.* Einaudi *et al.,* 1981; Ettlinger 1990; Ettlinger *et al.,* 1992; Meinert 1998). The characteristic presence of As and Bi in Au skarns (Meinert 1989; Theodore *et al.,* 1991; Ray and Webster 1995), as well as metal distributions of various other metals, have been examined for a number of skarn types using a variety of approaches—these skarns include Au skarn (*cf.* Ray *et al.,* 1988; Ray and Webster 1995), Cu skarn (*cf.* Theodore and Blake 1975; Atkinson and Einaudi 1978; Einaudi 1982; Meinert *et al.,* 1997), Zn skarn (*cf.* Yun and Einaudi 1982; Meinert 1987), and W skarn (*cf.* Soler 1980; Guy 1979; Fonteilles *et al.,* 1989). For example, Meinert *et al.,* (1997) used statistical analysis of approximately 13,000 individual assays from the Big Gossan Cu–Au skarn, Irian Jaya, to show increases of Cu, Au, Ag, Pb, Zn, As, and Co toward the top of the system, and increases of Mo with depth. At the Fortitude deposit, Nevada, geochemical investigations over the last 30 years have allowed documentation of district-scale and deposit-scale Cu, Au, Ag, Pb, and Zn zonations, as well as (1) the implications of Ag/Au ratios in rocks in the immediate area of the Fortitude, and (2) Ag/Au ratios in surrounding polymetallic veins. However, many other Au skarns are devoid of significant concentrations of Pb and Zn (Johnson 1991, 1992; Johnson and Meinert 1994).

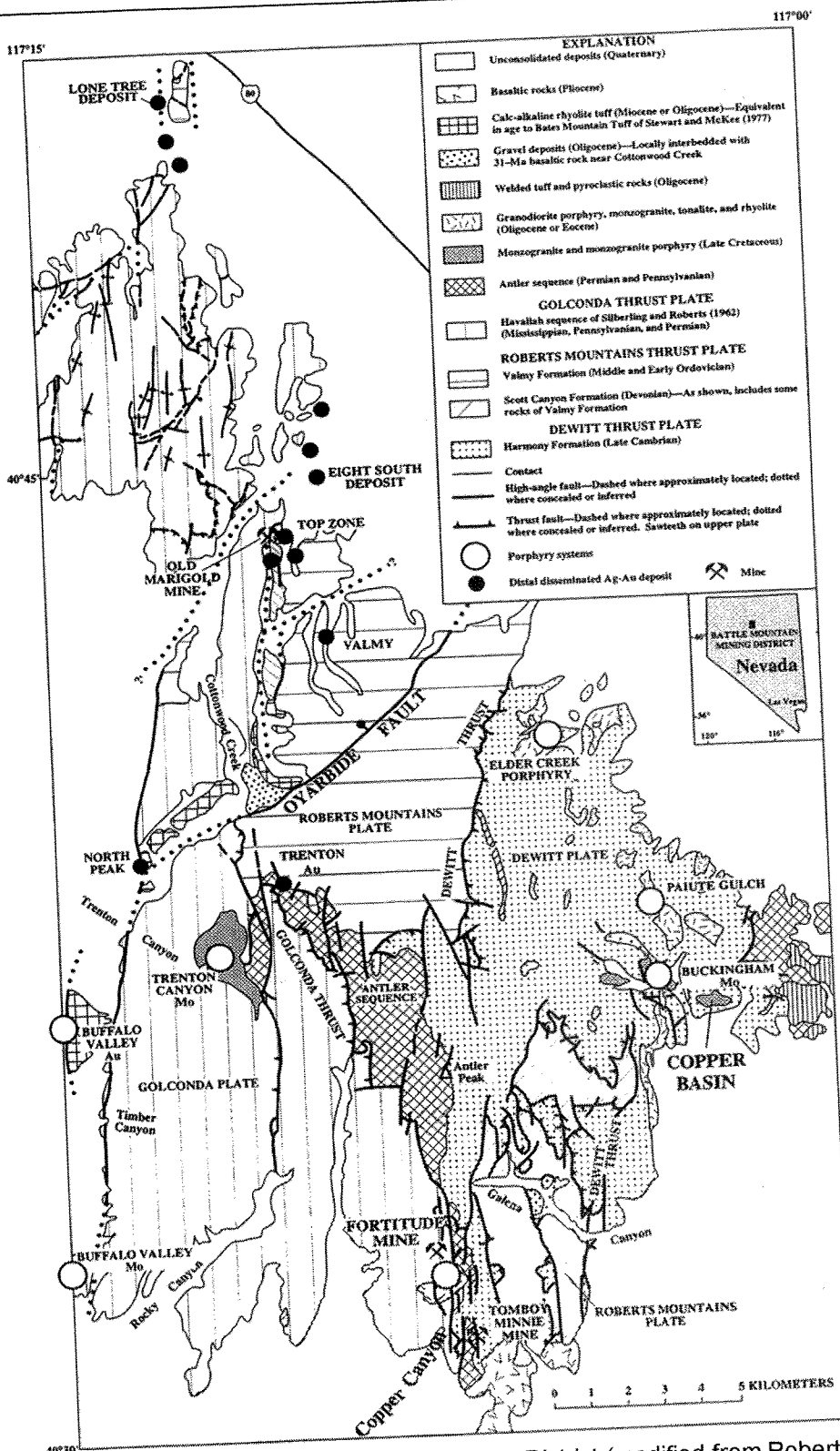

Figure 1: Geology of the Battle Mountain Mining District (modified from Roberts 1964, Theodore 1991, and Doebrich, 1995).

GEOLOGY

The Battle Mountain Mining District includes two major allochthonous terranes—one accreted during the late Devonian and (or) early Mississippian Antler orogeny, and the other during the latest Permian and (or) early Triassic Sonoma orogeny (**Fig. 1**; Roberts *et al.,* 1958; Silberling and Roberts 1962; Roberts 1964). The former includes the allochthon of the Roberts Mountains thrust, which, at Copper Canyon (**Fig.** 2), is made up of the Upper Cambrian Harmony accreted terrane is made up of the upper plate of the Golconda thrust, which includes strata belonging to the Mississippian, Pennsylvanian, and Permian Havallah sequence (**Fig.** 2; Murchey 1990).

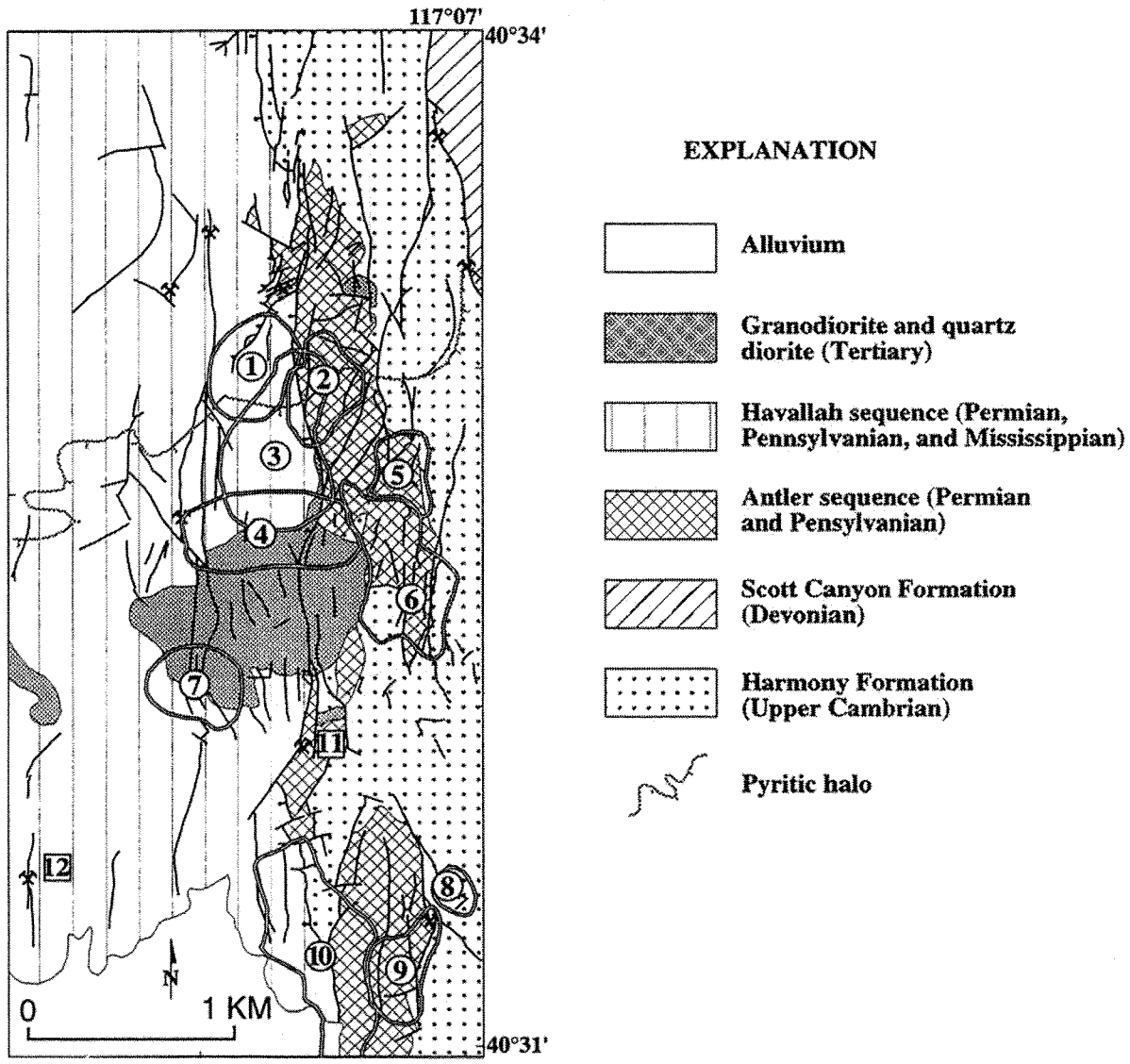

Figure 2: Geology of the Copper Canyon area (modified from Theodore and Blake 1975). Deposits nos. 1-12, deposits discussed in report. 1, Lower Fortitude; 2, Upper Fortitude; 3, Phoenix; 4, West orebody; 5, Northeast Extension; 6, East Orebody; 7, Reona; 8, Minnie; 9, Tomboy; 10, Midas; 11, Copper Canyon underground (Cu-Pb-Zn); 12, Wilson-Independence (Au-Ag). Deposits nos. in circles indicate large Au-Ag deposits mined by open-pit methods.

Major shortening in the upper plate of the Golconda thrust may have occurred along the Willow Creek thrust rather than the Golconda thrust (Theodore, 1999). An intervening block of autochthonous rock is present between the accreted terranes, and this block (Pennsylvanian and Permian Antler sequence) belongs to the overlap assemblage of Roberts (1964), and includes the Middle Pennsylvanian Battle Formation, the Pennsylvanian and Permian Antler Peak Limestone, and the Permian Edna Mountain Formation. The Antler Peak Limestone is the main host for mineralized skarn at Copper Canyon. At least seven centers of porphyry Cu (38–40 Ma) and stockwork Mo (86–90 Ma) mineralized rock are present in the mining district (**Fig. 1**), and a number of Tertiary distal-disseminated Ag–Au deposits (Cox and Singer 1992)—inferred to represent the tops of porphyry centers—are present mostly north of the Oyarbide Fault (700 m normal separation). These distal-disseminated Ag–Au deposits are northeast of the Cretaceous Trenton Canyon stockwork Mo system (Theodore *et al* 1992; Theodore 1996; Ivosevic and Theodore 1996; Doebrich and Theodore 1996). If one were to include porphyry systems probably buried under the Lone Tree and Marigold areas, then the mining district might include as many as nine porphyry systems (**Fig. 1**).Nonetheless, Myers (1994) initially recognized and documented the presence of distal Pb and Zn concentrations on the northern fringes of the Fortitude. In other parts of the world, Korobeinikov (1991) describes the intriguing presence of "above ore" (Ba, Hg, Sb), "near ore" (Cu, Pb, Zn, Bi, Te, Ag, As, W, Au), and "below ore" (Mn, Ti, Ni, V, Co, Cr, Mo, As) elements in vertical sections as much as hundreds of meters thick through Au–bearing contact metasomatic bodies in several mining districts in the Former Soviet Union. In addition, Beus and Grigorian (1977) categorize the primary dispersion haloes around a large number of types of deposits, including base- and precious-metal skarns. The Sarycheku skarnrelated porphyry Cu system, Uzbekistan, includes Cu–Au skarn that has a distal halo of Ag and Pb surrounding its proximal Cu plus Au zones. Meinert *et al.,* (1997) report the presence of a distal Pb–Zn halo on the fringes of the Big Gossan Cu–Au skarn deposit (37 million t (metric tonnes) at 1.02 g Au/t), Irian Jaya—a deposit which apparently also contains negligible amounts of As and Bi. At this deposit, Au, Pb, and Zn increase towards the margins of the deposit (*cf.* Rubin and Kyle 1997).

The primary purpose of this paper is to document the zonation of metals at various scales in the Battle Mountain Mining District, and, in particular, the three-dimensional zonation of metals at the Fortitude Au skarn. The metals for which enough three-dimensional data are available include Cu, Au, Ag, Pb, and Zn. This detailed analysis will help to improve petrogenetic models for the complex magmatic-hydrothermal evolution of these systems, as well as form the basis for understanding the zoning sequence and deposition processes for various types and styles of mineralization, and help develop better lithogeochemical exploration criteria. The Copper Canyon area may eventually achieve a proved geologic resource of approximately 380 t Au (12 million oz Au) when all near-surface orebodies have been delineated fully in the early 21st century (**Table 1**; Art Campo, oral communication, 1998).

The spatial and paragenetic sequence of calc-silicate alteration in the Battle Mountain Mining District is precisely the same as that present at the Hedley Mining District, British Columbia (*cf.* Ray and Dawson 1994), although at Battle Mountain many occurrences of skarn are not mineralized (Theodore and Hammarstrom 1991). At Battle Mountain, zonation outward from a garnet- dominant zone progresses through a pyroxene-dominant zone, which is followed by a narrow zone of K–feldspar alteration, and, finally, a zone of biotite hornfels alteration, wherein the former mineral assemblages overprint the latter ones in the succession. The spatial zonation of calc-silicate minerals around other mineralized skarn has been described in significant detail (Einaudi *et al.,* 1981; Meinert 1989; Casquet and Tornos 1991; Ray and Dawson 1994; Gray *et al.,* 1995; Mueller 1997; Meinert *et al.,* 1997; Meinert 1998).

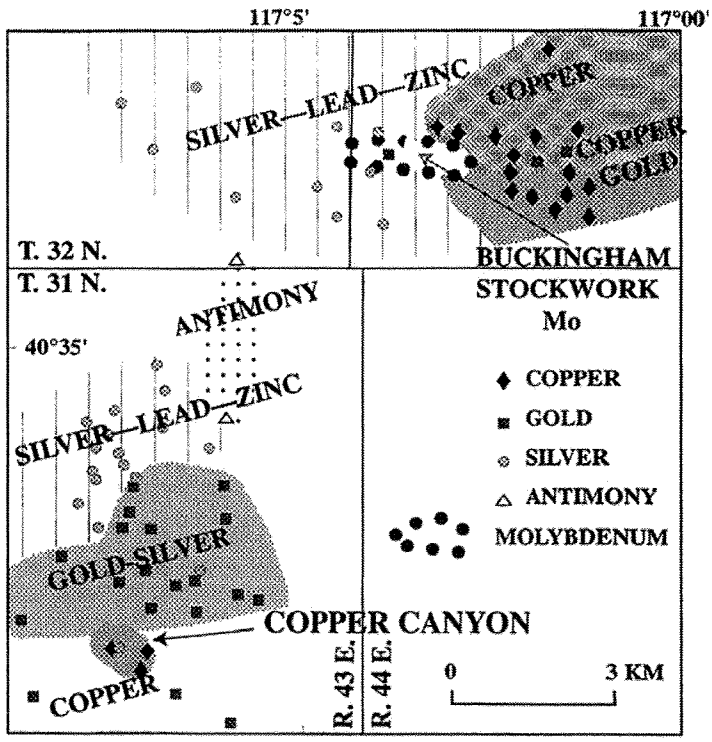

Figure 3: Metal zones in Battle Mountain Mining District established by Roberts and Arnold (1965) on the basis of major metal produced at each of the small mines in the mining district. Buckingham stockwork Mo deposit (Theodore et al. 1972), not recognized at time metal zones delineated, also is shown.

Most highly mineralized centers in the mining district are present at the intersections of a number of north- and northwest-trending structural zones (Doebrich and Theodore 1996). Copper Canyon area is the site of one of these structural intersections, which apparently provided the favorable structural setting for a 38 to 40 Ma granodioritic magma to be emplaced astride several major tectonic blocks (**Fig.** 2; *cf.* Theodore and Blake 1975). Porphyry-related mineralization at Copper Canyon evidently formed in a relatively shallow geologic setting (approximately 40 MPa or 1.5 km, Myers 1994).

MINING HISTORY

Historically, the Battle Mountain Mining District has been one of the largest producers of Cu, and since 1978 Au, in Nevada—mining in the district spans a period of more than 125 years (Theodore *et al.,* 1992; Doebrich *et al.,* 1996). The Copper Canyon Cu–Pb–Zn underground mine (deposit no. 11, **Fig.** 2) in the southern part of the mining district—one of the significant early sites for the production of metal—was operated sporadically between 1917 and 1955 (Roberts and Arnold 1965). However, the first large-scale attempt to mine base and precious metals by open-pit methods, mostly Cu, did not begin until 1967 in both the Copper Canyon and Copper Basin areas. At Copper Canyon, mining at that time was centered on the East Orebody (deposit no. 6, **Fig.** 2). Large-scale mining operations at Copper Canyon and Copper Basin center on porphyry-type mineralized rock that has widely divergent ages: about 39 Ma at Copper Canyon and 86 Ma at Copper Basin (McKee 1992). Copper in the Copper Basin area mostly is present in secondarilyenriched orebodies that fringe the Buckingham stockwork Mo deposit (Theodore *et al.,* 1992). The Fortitude gold skarn deposit is the most important Au orebody known to date in the Copper Canyon area (Wotruba *et al.,* 1986; Myers 1994; *cf.* **Table**

1). The Nevada Mine, now inaccessible, is a polymetallic replacement and vein occurrence hosted in rocks of the Antler sequence, which were exposed in a window through the Golconda thrust (Theodore and Blake 1975). The Nevada Mine produced about 273 oz Au and 28,000 oz Ag from 1902 to 1948 (Roberts and Arnold 1965).

The Copper Canyon area probably will eventually achieve a proved geologic resource of approximately 380 t Au (12 million oz Au) when all near-surface orebodies have been delineated fully in the early 21st century (**Table 1**). Depth of oxidation is quite shallow in the area, which makes it ideally suited for studies involving primary elemental dispersion haloes in the third dimension. In addition, the Fortitude deposit was not oxidized, and it included abundant pyrrhotite, chalcopyrite, marcasite, arsenopyrite, and pyrite, as well as a number of Bi– and Te–bearing minerals set in a hedenbergitic and andraditic silicate gangue that is variably altered to chlorite, epidote, and actinolite (Myers 1994).

Mining during 1997 in the Copper Canyon area was from the Midas oxidized Au–Ag skarn deposit (**Fig.** 2), where approximately 70,000 oz Au/yr were produced using cyanide heap leach technology. The Midas Au-Ag deposit, drilled in the late 1980s in the southern part of the Au–Ag zone delineated by Roberts and Arnold (1965) around the Copper Canyon area, is contained primarily in the Battle Formation. Feasibility and permitting work continues on the upcoming Phoenix Project. Annual production is projected to be 200,000 oz Au/yr, commencing by the year 2002. Project measured and indicated reserves, as of September 1999, stand at approximately 4,900,000 oz Au.

TABLE 1. Grade and tonnage of large Au–Ag deposits in Copper Canyon area, Nevada

Deposit no. (same as figs. 2, 14)	Name of deposit	Tonnage (short tons, X 10^{-6})	Gold (troy oz per ton)	Silver (troy oz per ton)
1.	Lower Fortitude	8.1	0.24	0.93
2.	Upper Fortitude	2.8	.08	.83
3.	Phoenix	42.6	.046	.26
4.	West Orebody[1]	5.	.012	.27
5.	Northeast Exten.	1.2	.07	.27
6.	East Orebody[1]	14.8	.012	.27
7.	Reona	8.2	.031	.22
8.	Minnie	. 7	.07	.12
9.	Tomboy	2.9	.07	.12
10.	Midas (Mill)	19.8	.047	.372
	(Leach)	8.6	.029	.214
11.	Sunshine	.43	.02	.15
	Total	115.		

Data represent production for deposit nos. 1, 2, 4, 5, 6, 8, and 9; and proven and (or) probable resourc for other deposits (modified from Doebrich *et al.*, 1996; Battle Mountain Gold Co., written communs., 1999).

[1]Byproduct production of Au and Ag from ores milled primarily for Cu content. In addition, approximately 0.07 million short tons Cu recovered from 47.8 million short tons placed on leach production dumps mined primarily from East and West Orebodies.

PREVIOUS GEOCHEMICAL STUDIES AT COPPER CANYON

As part of the U.S. Geological Survey's Heavy Metals Program of the late 1960s, 2,927 rock samples were collected and analyzed from outcrops in the Copper Canyon area (Theodore 1970; Theodore and Blake 1975). The material analyzed consisted of approximately 1 kg composite rock-chip samples each of which commonly was collected over an outcrop area of approximately 10 square meters. These samples were analyzed for 30 elements by emission spectrographic methods (Grimes and Marranzino 1968), and for Au and Hg by atomic absorption and a cold-vapor atomic absorption procedure, respectively (Haffty *et al.,* 1977; Wilson *et al.,* 1987). A report by Theodore (1969) shows the surface distribution of 20 elements at the respective sampling sites, classified according to numerical intervals determined largely from breaks in elemental distributions noted in histograms prepared from data obtained from the northern, least altered third of the Copper Canyon area. The northern part of the Copper Canyon is largely beyond the pyritic halo, within which rocks are converted to hornfels and are sulfidized around the altered granodiorites (**Fig.** 2), and thus relatively free of epigenetic metals. The 2,927 samples that comprise the surface lithogeochemical data base can be categorized approximately as follows: 32% Havallah sequence, 7.7% altered granodiorite, 17% Harmony Formation, 11.6% fault breccia, 10.6% gossan (mostly along faults), 11.7% Battle Formation, and 8.4% undivided hornfels.

Various aspects of rock geochemistry at Copper Canyon are described by Theodore and Nash (1973), Theodore and Blake (1975, 1978), and Theodore *et al.* (1986). The only widespread disturbance of the ground at the time of sampling in 1968 was in the immediate area of the East Orebody (**Fig.** 2), which is a Cu–Au–Ag replacement body formed in the Middle Pennsylvanian Battle and Upper Cambrian Harmony Formations (Theodore and Blake 1975). In addition, Theodore and Nash (1973) showed a crude zonal pattern of metal distributions centering on the altered granodiorite of Copper Canyon. Molybdenum is confined tightly to the altered granodiorite of Copper Canyon, and the various other metals were interpreted to be present in the wallrocks of the altered granodiorite at various concentrations and at various places.

Samples from drill holes represent 5 ft (1.52 m) and (or) 10 ft (3.04 m) channel samples and were analyzed for Cu, Au, Ag, Pb, and Zn by atomic absorption methods on site in the laboratories of Battle Mountain Gold Co., and classified according to host rock and position in three-dimensional space. The 982 samples that comprise the drill core data base can be categorized approximately as follows: 25.6% Havallah sequence hornfels, 44.3% skarn (from Antler Peak Limestone and Edna Mountain Formation), 7.5% ore (also skarn), 21.7% Battle Formation hornfels, and 0.9% altered granodiorite.

GEOCHEMISTRY OF SURFACE ROCKS AT COPPER CANYON

From the original 2,927 samples, data for 2,708 samples were extracted and interpolated to a square grid by means of a routine based on the principal of minimum curvature (Briggs 1974; *cf.* Kotlyar *et al.,* 1995). The gridding procedures employed are relatively sensitive to the density and uniformity of sampling sites in small domains, which, however, does not result in total disappearance of anomalies nor in the appearance of spurious anomalies. Nonetheless, presence of a large number of samples with relatively low concentrations in a domain surrounding a small number of samples with high concentrations of that element can result in severe damping of the level of the anomaly. In addition, the gridded map data were spatially filtered in an effort to emphasize the broad ("long-wave Geological length") characteristics of the geochemical anomalies by suppressing the narrow ("short wavelength") components (Kotlyar *et al.,* 1995). With the specific filter used, the shorter the wavelength, the greater the suppression. The magnitude of the relative suppression between any two wavelengths is controlled in this filter by a free parameter *z*, which has dimensions of length. Short-wavelength characteristics of the data are more strongly attenuated by filters with large values of *z*. Thus, filters with large

values of *z* are more effective in emphasizing long-wavelength characteristics of anomalies. The type of filter used in this study, when applied to gravity or magnetic data, is known as the "upward continuation" filter (Blakely 1994), because for a given value of *z*, the filtered data appear as if they had been measured on a surface that is distance *z* above the original data surface. The computer-based filtering used in our study is quite analogous to the visual filter applied to down-hole geochemical data by Chaffee (1982).

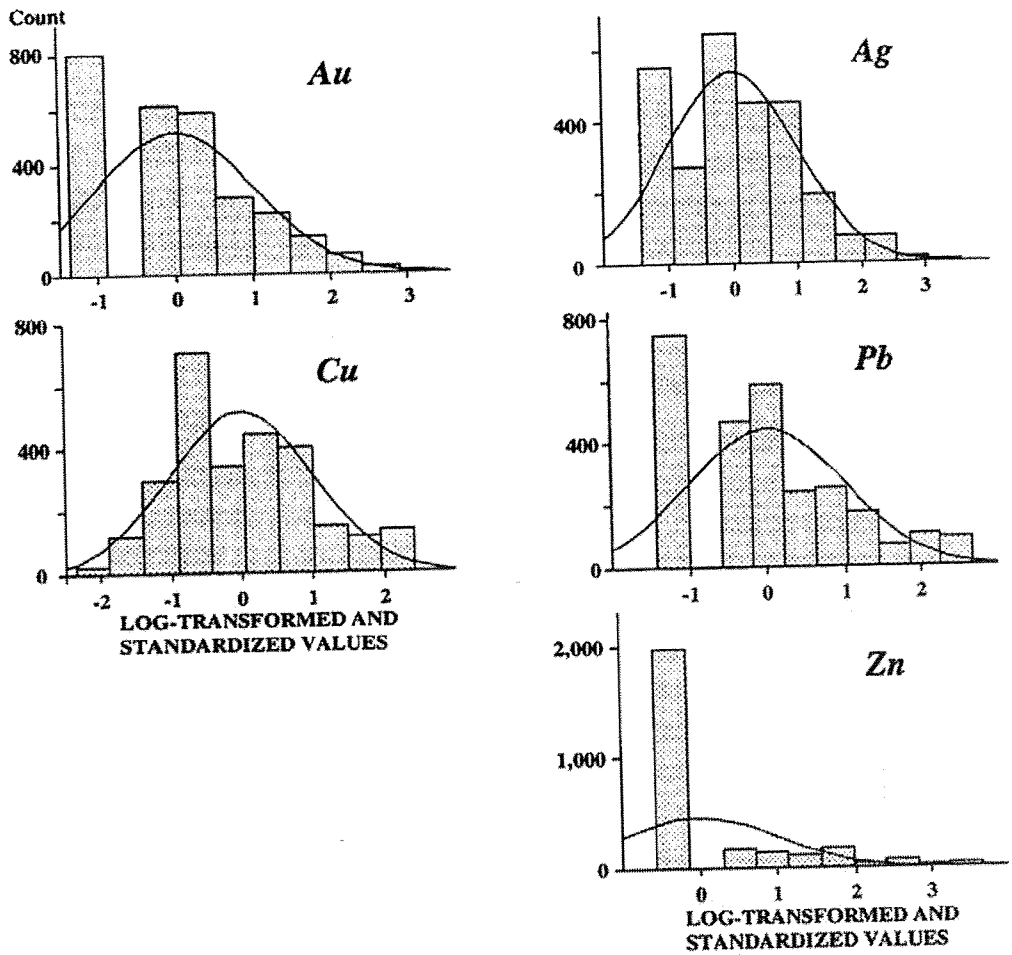

Figure 4. Frequency distribution of normalized logs of base and precious metals in surface samples (n = 2,708). Log-transformed data are standardized to standard deviations (see text).

Frequency distributions of normalized logs of concentrations for Au, Ag, Cu, Pb, and Zn in the 2,708–sample data set suggest that the sample population is strongly unimodal for Au, Ag, and Cu. Distributions for other metals are skewed, because large numbers of analyses were below detection levels (**Fig. 4**). We substituted 1 ppm, 1 ppm, 40 ppm, 0.1 ppm, and 0.002 ppm for the lower undetected values of Cu, Pb, Zn, Ag, and Au, respectively (**Table 2**). Approximately 70 analyses are greater than the upper determination limit of Cu, 30 greater than the limit for Pb, and 10 for Zn (Theodore and Blake 1975), for which we substituted 20,001 ppm Cu, 20,001 ppm Pb, and 10,000 ppm Zn.

A logarithmic transformation was used, because small but important variation may be compressed into a relatively narrow range, whereas other variation is spread out over a wider range than its importance justifies (Masters 1993). Another reason to transform the data is that tests of significance of Pearson product correlation coefficients are not valid for skewed

distributions. For each element, the transformed values were standardized or normalized to a Z–score by subtracting the subset's mean and dividing by its standard deviation. This removes all effects of different means and measurement scales and facilitates the comparison of the spatial patterns of the elements. Normalization of the data involved calculation of $(X_c - X_{mean})/X_{standard\ deviation}$, where all values are logarithms and X_c is the concentration for a selected element in an analyzed sample.

Various descriptive statistics in the transformed database used to generate the elemental distribution diagrams below are given in **Table 3**. The specific filter used in our study of the geochemistry of surface rocks employed a *z* factor equal to 200 m, and 50–m-wide grid cells.

Computer-contoured plots for Au, Cu, Ag, Pb, and Zn (**Fig. 5**) show systematic variations with respect to the pyritic halo and the surface projection of a number of large ore bodies that were unexposed in the area at the time of geochemical sampling, as well as the East Orebody. Locations of actual sampling sites are shown in **Figure 5*B***. High concentrations of Cu largely reflect the area of outcrop of altered Copper Canyon granodiorite; concentrations have been enhanced by supergene, downslope migration of Cu from the once topographically high East Orebody (deposit no. 6, **Fig. 5**; Theodore and Blake 1975). The highest concentrations of Cu (>500 ppm Cu, Kotlyar *et al.,* 1995) are somewhat broader than the large area enclosed by the 0.75s contour south-southwest of the East Orebody (**Fig. 5*C***). In addition, elevated abundance of Cu (0 to 0.25□, **Fig. 5*C***) is present in the general area of the Wilson-Independence Mine (deposit no. 12) and near a number of small exposures of altered Copper Canyon granodiorite approximately 500 m farther to the north.

TABLE 2. Descriptive statistics of 2708 surface samples, Copper Canyon, Battle Mountain Mining District, Nevada.

Parameters	Au	Cu	Ag	Pb	Zn
Descriptive Statistics (Raw data, in ppm)					
Mean	0.55	1259.	12.9	810.	324.
Std. Dev.	2.62	3767.	58.2	3066.	1007.
Std. Error	0.05	72.	1.12	58.	19.
Minimum	0.002	1.	0.1	1.	40.
Maximum	75.00	20001.	1500.	20001.	10000.
Skewness	14.74	4.15	12.68	5.16	6.55
Kurtosis	317.63	16.77	230.23	27.33	50.56
Descriptive Statistics (logs)					
Mean	-1.38	2.10	0.18	1.49	1.92
Std. Dev.	0.98	0.90	0.84	1.05	0.57
Std. Error	0.02	0.02	0.02	0.02	0.01
Minimum	-2.70	0.00	-1.00	0.00	1.60
Maximum	1.88	4.30	3.18	4.30	4.00
Skewness	0.34	0.54	0.40	0.75	1.60
Kurtosis	-0.50	-0.23	-0.12	-0.04	1.52
Descriptive Statistics (normalized data:(logx-logmean)/logStd.Dev.)					
Mean	0.00	0.00	0.00	0.00	0.00
Std. Dev.	1.00	1.00	1.00	1.00	1.00
Std. Error	0.02	0.02	0.02	0.02	0.02
Minimum	-1.35	-2.34	-1.40	-1.42	-0.56
Maximum	3.34	2.44	3.56	2.68	3.68
Skewness	0.34	0.54	0.40	0.75	1.60
Kurtosis	-0.50	-0.23	-0.12	-0.04	1.52

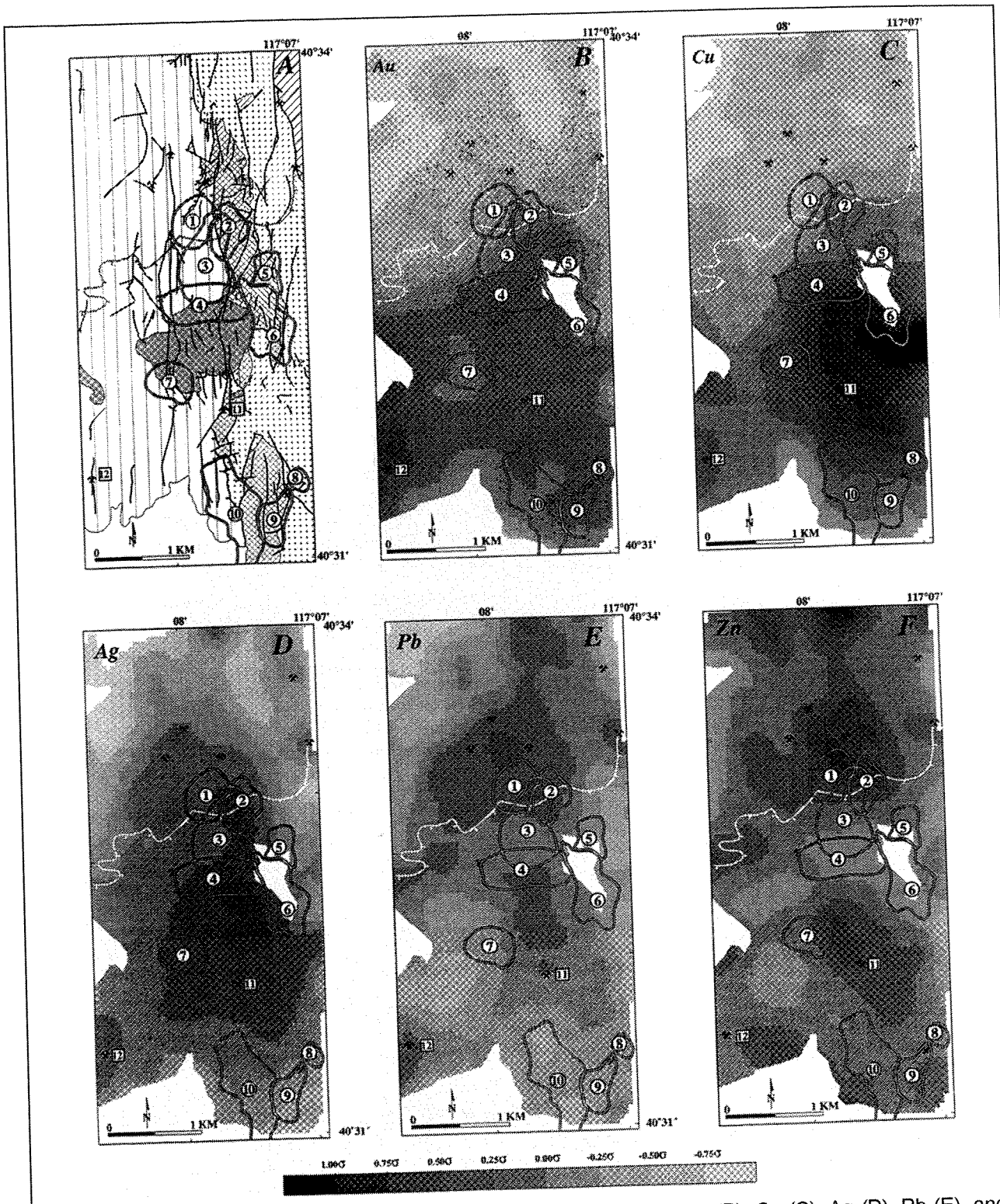

Figure 5: Geology (A) and distribution of normalized log contents for Au (B), Cu (C), Ag (D), Pb (E), and Zn (F) in 2,708 rock samples. Explanations for A same as **Figure 2**. Dots on B, sample localities of analyzed samples. Reported metal contents gridded and filtered (see text), resulting in contours showing standard deviations (s) of metal concentrations from mean – more densely shaded patterns are higher standard deviations. Unpatterned, areas without rock samples. Deposit numbers as same as **Figure 2**.

The level of abundance of Cu in these small exposures probably results from in-place secondary Cu derived from disseminated hypogene chalcopyrite present in potassically altered-granodiorite. The computer-contoured plots for Au, Cu, and Ag (**Fig. 5*B–D***) all show that most of the high values are located within the pyritic halo, which surrounds the mineralized porphyry system at Copper Canyon. The southern part of the halo largely is covered by Tertiary and Quaternary unconsolidated deposits. In addition, Ag is elevated in relatively small areas surrounding polymetallic veins located north of the pyritic halo (**Fig. 5*D***). Overall, distribution of Ag defines a broad high that is elongated north-south, and apparently extends as much as 1 km beyond the pyritic halo (**Fig. 5*D***). However, many of the samples with high Pb and Zn contents are outside the pyritic halo (**Fig. 5*E–F***), whereas strongly anomalous Zn (0 to 0.25σ) inside the pyritic halo is present in the general area of the Copper Canyon underground mine (deposit no. 11, **Fig. 5*F***), which had notable concentrations of sphalerite and galena in its 700–ft levels (Roberts and Arnold 1965). Thus, metal haloes at the surface occupy well-defined distal and proximal positions to the orebodies as described in more detail below.

GEOCHEMISTRY OF DRILL-HOLE SAMPLES FROM FORTITUDE AU SKARN DEPOSIT

From a large number of drill holes in the general area of the Fortitude deposit (open circles, **Fig. 6**), 982 samples were selected for study of the distributions of Cu, Au, Ag, Pb, and Zn. The samples were taken from ten drill holes close to a north-south section through the Fortitude deposit (**Fig. 6**). Drill holes 3101 and 2753 (**Fig. 6**) provide convenient reference points in many figures that follow.

Histograms of normalized logs for Au, Cu, Ag, Pb, and Zn concentrations (**Fig. 7**) in 982 mostly unoxidized samples show unimodal distributions whose modes compare remarkably well with modes for the largely oxidized 2,708 surface samples analyzed in the Copper Canyon area (*cf.* **Figs. 4** and **7**). A notable difference, however, is the lack of a low value peak for Zn for the data from the drill holes surrounding the Fortitude. This relation probably reflects the relatively high detection limit for Zn in the original data base for the surface rocks (200 ppm Zn, Theodore and Blake 1975), as well as a generally higher threshold concentration for Zn in the rocks around the Fortitude.

Gold-skarn mineralized rocks in the Lower Fortitude, which were not exposed prior to mining, are restricted largely to the generally flat-lying Pennsylvanian and Permian Antler Peak Limestone—the middle formation of the Antler sequence present below the Golconda thrust. These rocks extend at depth below the Golconda thrust as much as 1,000 m from the northern contact of the granodiorite (**Fig. 8**; *cf.* Wotruba *et al.,* 1986; Myers 1994). Along section AA', two orebodies comprise the Lower Fortitude Au skarn: orebody I, proximal to the altered granodiorite of Copper Canyon, and II, distal from it (**Fig. 8*A***). Mineralized rocks formed in a relatively shallow-seated geologic setting (approximately 40 MPa or roughly 1.5 km paleodepth, Myers, 1994; *cf.* Nash and Theodore 1971; Theodore and Blake 1975). Two other orebodies also are present in this package of rocks along the north-south section. The West Cu–Au–Ag orebody (**Table 1**), adjacent to the altered granodiorites of Copper Canyon, was mined in the 1970s (Theodore and Blake 1978), and the Phoenix deposit, which is being prepared for production (Doebrich *et al.,* 1996). Orientation of these generally flat-lying orebodies reflects the premineralization geometry of the Antler sequence beneath the Golconda thrust. Overall geometry of these orebodies at Copper Canyon (**Fig. 8**) is similar to that at the Junction Reefs deposits, New South Wales (Gray *et al.,* 1995). Some penetration of mineralizing fluids into the relatively impervious argillite and chert in the upper plate of the Golconda thrust occurred, as exemplified by presence of a number of small vein deposits and occurrences in upper plate rocks (Roberts and Arnold 1965; Theodore and Blake 1975). The Virgin Fault is a high-angle fault that dips steeply to the west yielding a horizontal trace on the plane of the cross section (**Fig. 8*A***).

Table 3. Descriptive statistics of 982 drill-hole samples of along section AA' through Fortitude deposit, Battle Mountain Mining District, Nevada.

Parameters	Au	Cu	Ag	Pb	Zn
Descriptive Statistics (Raw data, in ppm)					
Mean	2.55	574.	11.9	214.	379.
Std. Dev.	10.39	1500.	27.4	485.	2225.
Std. Error	0.33	47.8	0.88	15.5	71.
Minimum	0.01	50.	0.14	4.	4.
Maximum	146.25	19600.	359.	6100.	67500.00
Skewness	7.71	5.76	5.25	6.91	28.06
Kurtosis	77.35	44.28	40.86	61.09	841.07
Descriptive Statistics (logs)					
Mean	-0.72	2.25	0.55	1.97	2.12
Std. Dev.	0.89	0.56	0.63	0.52	0.56
Std. Error	0.03	0.02	0.02	0.02	0.02
Minimum	-1.85	1.70	-0.85	0.60	0.60
Maximum	2.17	4.29	2.56	3.79	4.83
Skewness	0.81	1.13	0.58	0.39	0.39
Kurtosis	0.19	0.65	0.10	0.29	0.30
Descriptive Statistics (normalized data:(logx-logmean)/logStd.Dev.)					
Mean	0.00	0.00	0.00	0.00	0.00
Std. Dev.	1.00	1.00	1.00	1.00	1.00
Std. Error	0.03	0.03	0.03	0.03	0.03
Minimum	-1.27	-0.97	-2.22	-2.62	-2.72
Maximum	3.25	3.63	3.19	3.49	4.86
Skewness	0.81	1.13	0.58	0.39	0.39
Kurtosis	0.19	0.65	0.10	0.29	0.30

Down-hole gridding and filtering procedures then were used to establish loci of Au, Cu, Ag, Pb, and Zn metallization along a north-south section (AA', **Fig. 6**) through the Lower Fortitude (**Fig. 8**). The "Au" symbol, for example, is placed visually at the center of gravity of normalized gridded and filtered data for Au—contours are in standard deviations, darker gray shades indicate higher positive deviation from the mean Au content across the plane of the section. Normalization procedures employed are the same as those applied to the surface rock geochemical data (see above). The locus of Au metallization along the section is compared with loci of other metals, established using the same technique, and shows a progression respectively from south to north (AA', **Fig. 8**) of Au, Cu, Ag, Pb, and Zn loci of metallization. These loci are generally coincident with the projected trace of the Lower Fortitude orebody onto the cross section—the locus for Au is at the south end of the orebody (**Fig. 8*A***), that is, proximal to the granodiorite of Copper Canyon, and Zn is at the distal end (**Fig. 8*F***). A lower level Au anomaly also is present below the Lower Fortitude, and this lower anomaly comprises two parts: (1) a mushroom-shaped oblong part elongated north-south, and (2) a pillar-shaped part which connects the lower anomaly with Au concen trations centered just below the Lower Fortitude (**Fig.** 8*B*). In contrast to the other metals, two widely separate loci of equally intense Pb–mineralized rocks are present along the section: an upper one that may be arcuate shaped with parts removed by erosion above the north end of the Lower Fortitude—our preferred interpretation—and a lower one that is mushroom shaped deep below the Lower Fortitude and connected to the upper anomaly by a pillarshaped part (**Fig. 8*E***). This lower level Pb anomaly below the Fortitude is spatially associated with the lower level Au anomaly.

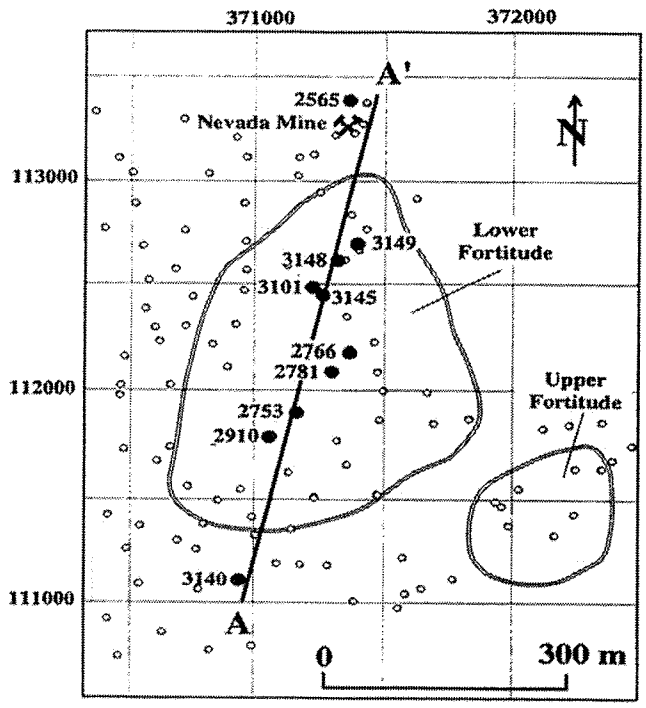

Figure 6: Surface projection of Lower and Upper Fortitude orebodies together with locations of selected drillholes and line of section A-A'. Difference in shape of Upper Fortitude here compared to Figure 2 results from the fact that the outer limit of the open pit is shown on Figure 2. Drillhole numbers same as Figures 7, and 11-13. Solid dots, diamond drillhole data for Au, Cu, Ag, Pb, Zn projected to section A-A': open circles, additional exploration drillholes in area of Fortitude. Grid based on Battle Mountain Gold Co. coordinates.

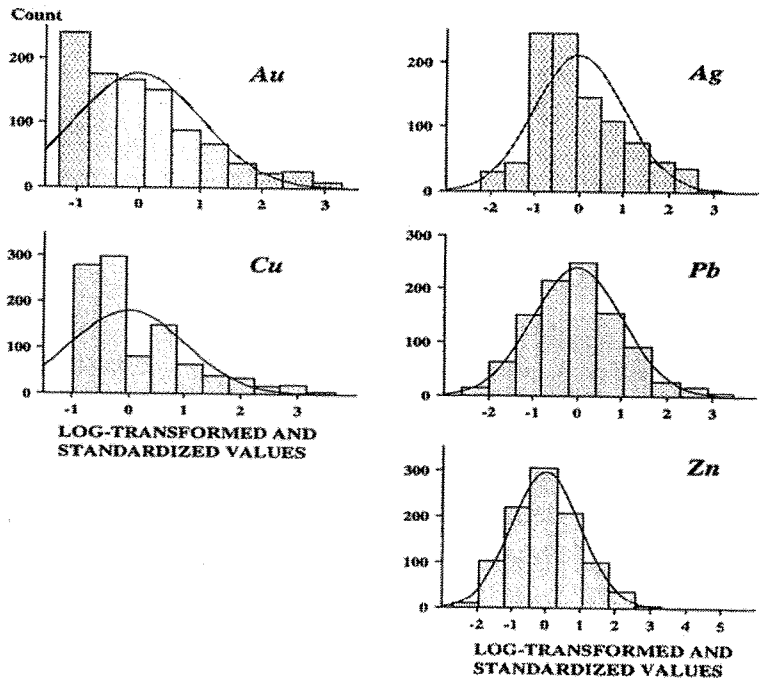

Figure 7: Frequency distributions of normalized logs of base and precious metals in core samples (n = 982). Log-transformed data are standardized to standard deviations (see text).

A three-dimensional configuration of gold-metallized rock in the southern parts of the Lower and Upper Fortitude deposits was constructed on the basis of Au contents in a large number of exploration holes (**Fig. 9**). The 1 ppm Au outer halo that surrounds the Fortitude is much more complex than previously envisioned—compare with **Figure 8*A***—and geometry of this halo primarily reflects distribution of chemically receptive rocks in the premineral calcareous Antler sequence below the Golconda thrust. These rocks were broken and displaced predominantly by normal movements along the Virgin Fault (**Fig. 8*A***) and numerous other penecontemporaneous north-south striking faults in the Copper Canyon area (**Fig. 5*A***). Most Au in the deposits is present as separate free phases, including electrum (Theodore *et al.*, 1991; Myers 1994), but many of the abundant sulfide minerals in the deposit—including arsenopyrite, pyrrhotite, chalcopyrite, pyrite, marcasite, galena, sphalerite, and several Bi–bearing phases—undoubtedly contain some unknown amount of Au in their crystal lattices (*cf.* Cabri *et al.*, 1989; Harris 1990).

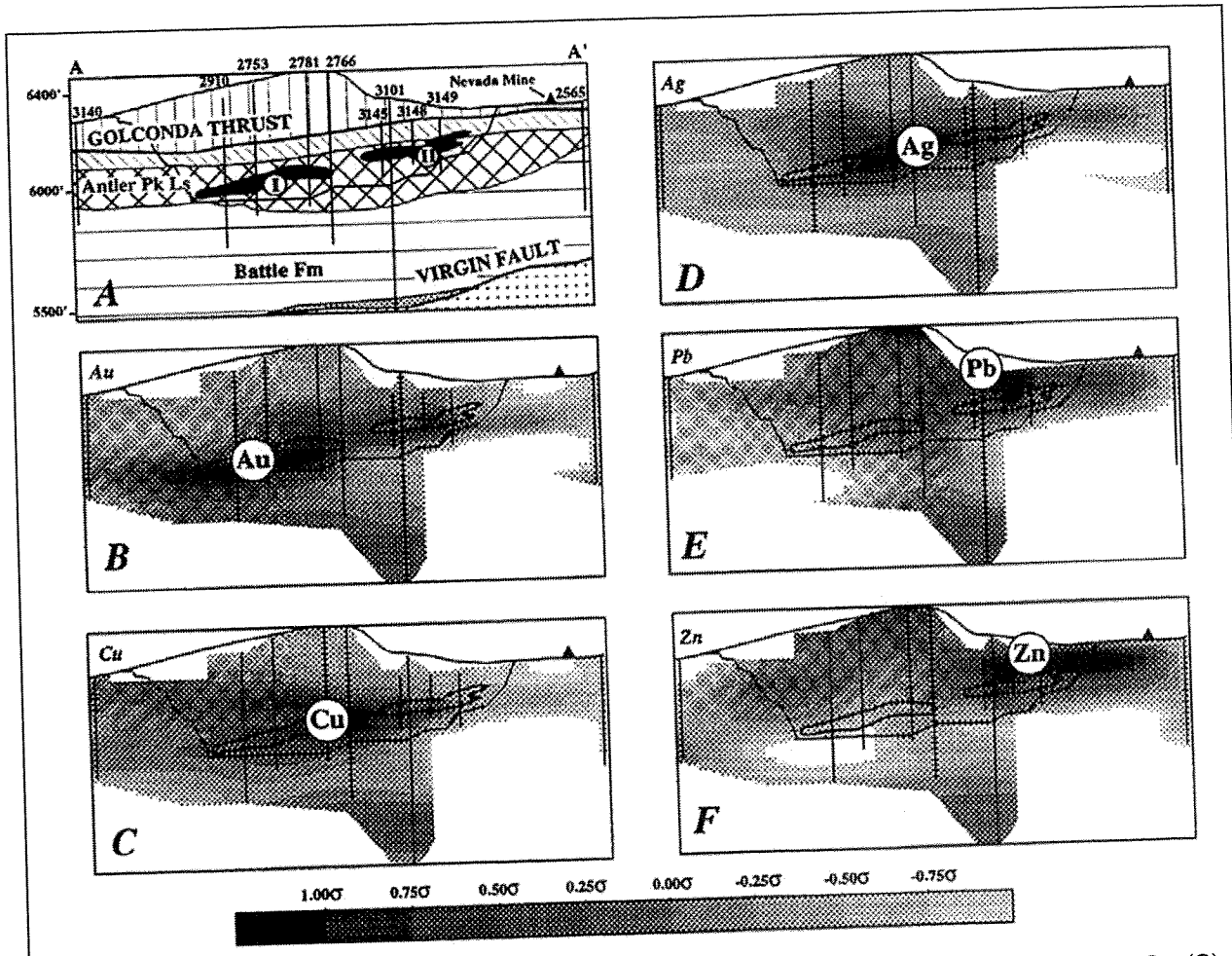

Figure 8: Geology (A) and normalized, gridded and filtered (see text) distributions of Au (B), Cu (C), Ag (D), Pb (E), and Zn (F) in Section AA' (**Figure 6**). Explanation for A same as **Figure 2**: black, projection of ore in Lower Fortitude to plane of section. More densely shaded patterns (in B-F) represent higher deviations from the mean distribution. Circled chemical symbols represent loci for most intensely concentrated presence of proximal (Cu, Au, Ag) and distal metals (Pb, Zn). I, Southern orebody of Lower Fortitude: II, Northern orebody of Lower Fortitude.

Down-hole metal distributions and anomalies at Fortitude also were evaluated by a number of other methods. To demonstrate that down-hole metal distributions which comprise these multilevel anomalies are not artifacts of the contouring procedures used in our study, raw data

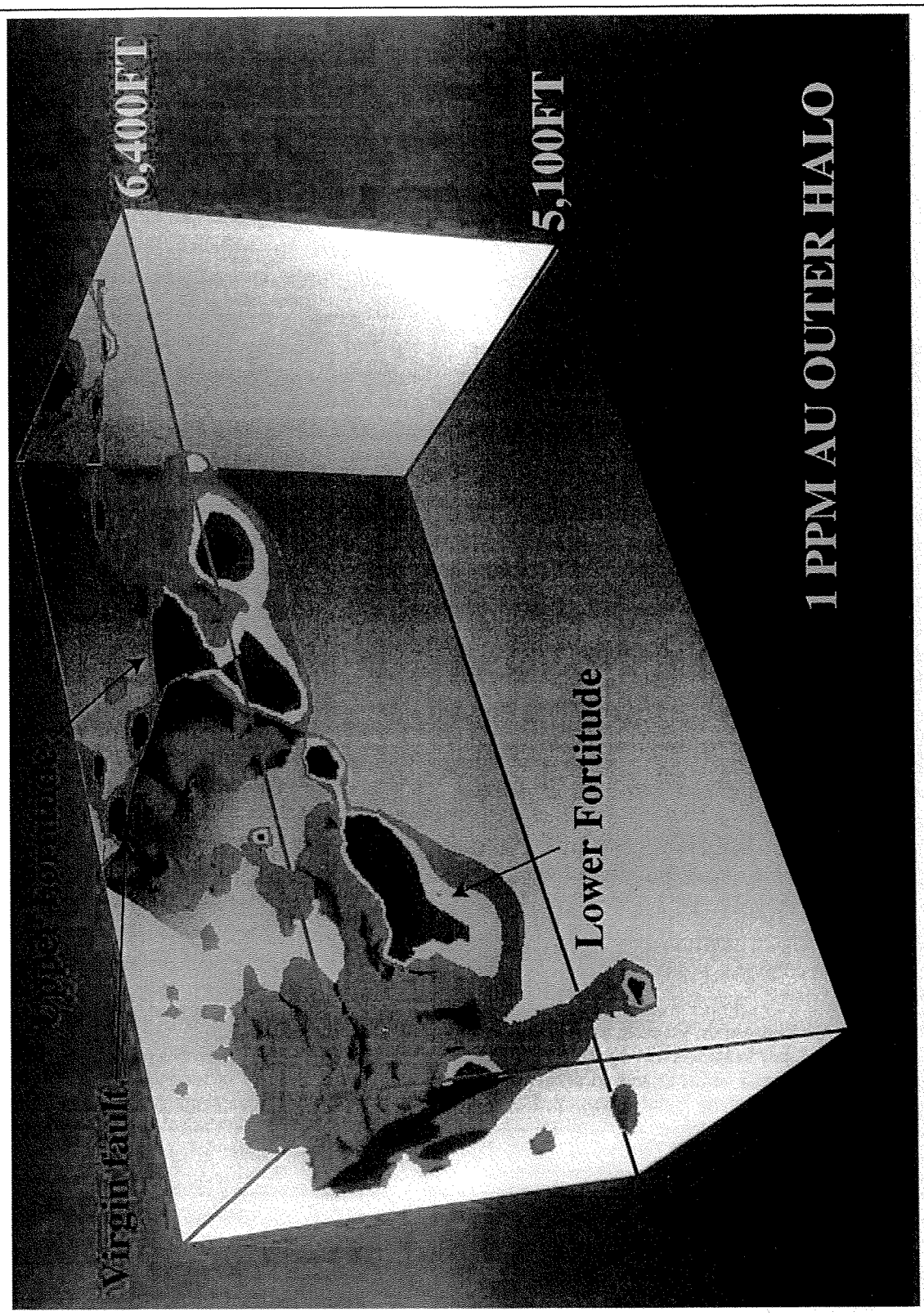

Figure 9: Block diagram showing three-dimensional configuration of roughly southern one-third of Lower and Upper Fortitude Au skarn orebodies and approximate trace of Virgin fault. Depicted outermost halo comprises 1 ppm Au.

for Au, Cu, Ag, Pb, and Zn are shown for two drill holes along the section (DDHs 3101 and 2753, **Fig. 10**). Further evaluation of loci of metallization (**Fig. 8**) with rigorously placed loci using log-transformed and standardized metal values summed over the mineralized intervals in eight of the drill holes along section AA' also was attempted (**Fig. 11**). Relative position of individual points on this figure does not represent absolute concentration of a metal, but rather the abundance of the metal normalized to its standard deviation in the 982 samples (see above). The relative positions of all five metal loci remain the same, although loci for Au, Cu, and Ag shift slightly to the north when examined using the latter procedures. In addition, values for (Au+Cu+Ag) – (Pb+Zn) (*cf.* Myers 1994) peak at approximately the same place along the profile as the Au and Cu loci, and then they decline markedly to the north along the profile (**Fig. 11**).

The distribution of values of Ag/Au weight ratios from drill holes along profile AA' through the Fortitude deposit provides additional insight into the process of metallization (**Fig. 12**). Much of the mineralized halo in siliceous rocks around Fortitude has Ag/Au weight ratios of 50 to 100—orange pattern (**Fig. 12**)—whereas Fortitude itself is marked by Ag/Au weight ratios approximately <10—pink pattern. Production of Ag and Au from the Lower and Upper Fortitude deposits amounted to 9,800,000 oz Ag and 2,100,000 oz Au respectively for a Ag/Au weight ratio of 4.6 for the deposits (Doebrich *et al.,* 1996). Utilization of production data as a signature of the deposit must be done judiciously, because these data probably are skewed markedly from their total values due to extractive methods used to maximize recovery of Au—much of the Ag in the deposit was in chalcopyrite and not recovered. These data nonetheless confirm Einaudi's (1990) conclusions about such ratios in Au–Ag orebodies in pluton-related environments: namely, orebodies in such geologic environments typically are marked by Ag/Au weight ratios less than 10, partly a reflection of the lower overall abundance of Au and the fact that Ag is much more soluble than Au as chloride complexes over a wide temperature range (Gammons and Williams-Jones, 1995). However, as well exemplified by down-hole Ag/Au weight ratios through the Fortitude and its surrounding halo of subeconomic-mineralized rock, extreme caution should be exercised about possibility of abrupt changes of Ag/Au weight ratios as premetallization lithology varies near these types of orebodies—especially changes from largely siliceous protoliths to largely calcareous ones. Rocks can have Ag/Au weight ratios much greater than 50 on the fringes of ore that has Ag/Au weight ratios approximately equal to 1.

Correlation coefficients (*r*) of logarithmic data also were examined in mineralized rocks surrounding Fortitude to determine zonal variability of *r* and potential impacts on classification schemes. Correlation coefficients for Cu–Zn, Cu–Pb, Pb–Ag, Zn–Ag, Pb–Au, and Zn–Au (shaded light gray) from the 982 samples in eight drill holes are not significantly different from zero along the projected north-south trace of Fortitude (**Fig. 13**). However, on the basis of comparisons of distributions of Cu and Au contents in mineralized rock surrounding the Lower Fortitude orebodies, Cu–Au correlations must vary significantly (**Fig. 8**). Cu and Au correlations have relatively low correlations in the southern part of the proximal orebody, whereas in the northern part of this orebody, Cu–Au correlations appear to be stronger (orebody I, **Fig. 8**). As a confirmation, calculated values of *r* for Cu–Au in mineralized rocks surrounding Fortitude, reach 0.6 in mineralized rock near the locus of highest Cu content, which coincides with the proximal orebody (orebody I, **Fig.** 8) of the two orebodies that comprise Lower Fortitude (**Fig. 13**). In the area of the distal orebody (orebody II, **Fig. 8**), values of *r* for Cu–Au are as high as 0.8. Nonetheless, approximately 80 percent of drill-hole intercepts into the Fortitude and its surrounding rocks yield Cu–Au correlation coefficients >0.4 (**Fig. 13**). These Cu–Au correlations are compatible with petrographic observations. Free Au is present commonly enclosed within chalcopyrite—particularly where the matrix of garnet skarn is replaced massively by chalcopyrite and pyrrhotite (*cf.* Myers 1994; Doebrich *et al.,* 1996). In addition, Ag–Au correlation coefficients progressively increase laterally outward from the Fortitude and reach their highest values well beyond the northern limits of the orebody, more or less in sympathy to a similar progressive

increase to the north in Pb–Zn Pearson product correlation coefficients (**Fig. 13**). These results demonstrate the significant problems of a deposit-type classification scheme that is based on ratios of correlations of elements in chemically complex systems. Because of spatial zoning of elements in many deposits, correlations or metal ratios in one part of the deposit typically are quite different than in another surrounding part.

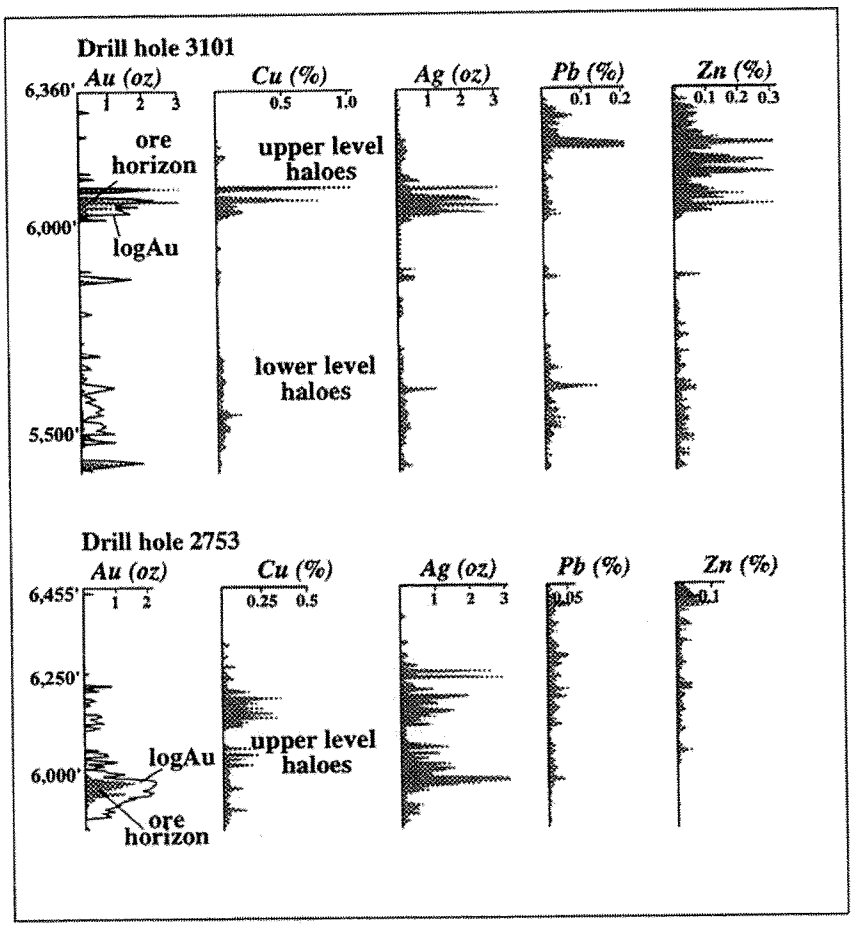

Figure 10: Geochemistry of diamond drill holes 3101 and 2753 showing details of metal distributions that comprise upper and lower geochemical halos along section AA'. See Figure 6 for location of drill holes 3101 and 2753.

DISTRICT-SCALE vs. DEPOSIT-SCALE METAL ZONATIONS

Metal zonations at Copper Canyon vary according to scale. Roberts and Arnold (1965) established that patterns of mining district-scale metal zonation are centered at Copper Canyon and Copper Basin on the basis of a broad distribution of polymetallic veins that had varying amounts of metal production (**Fig. 14**). Roberts and Arnold (1965) classified these polymetallic veins according to the dominant metal produced. However, the large stockwork Mo system at Buckingham (**Fig. 1**), containing resources of as much as 1.4 billion tons at 0.05 wt.% Mo, was not recognized at that time (Loucks and Johnson 1992; Theodore *et al.*, 1992).

Our evaluation revealed concentration of Au and Cu in the proximal parts of the system, as well as the presence of relatively steep declining concentration gradients of these metals northward at the pyritic halo that surrounds the Copper Canyon system (**Fig. 14**). Silver has a more diffuse pattern than Cu and Au, and is somewhat elongate in a north-south direction, straddling the pyritic halo. The bulk of the Pb and Zn are outside the pyritic halo, although substantial

concentrations of Pb and Zn are present near the Copper Canyon Cu–Pb–Zn underground mine (deposit no. 11, **Fig. 14**). These elevated contents of Pb and Zn might represent the leading edge of mineralized rock centered at the Midas deposit (deposit no. 10, **Fig. 14**). Reversal of the district-wide metal zoning pattern at the Tomboy-Minnie deposits (deposit nos. 8, 9; **Fig. 15**) (Theodore *et al.,* 1986) also might be a reflection of a focus of fluid influx at the Midas deposit into the Copper Canyon system as the system evolved. Indeed, at a much larger scale, district-wide geochemical patterns are confined tightly around Fortitude Au skarn as well as at some of the other Au skarn deposits (for example, Tomboy-Minnie deposits); Fortitude is close to the transition between Cu–Au–Ag and Pb–Zn zones (**Fig.** 8). District-scale metal zones are similar spatially to those at Bingham Canyon, Utah, except that at Bingham Canyon production from all metal zones has been significantly larger than at Copper Canyon (Einaudi 1982). Further evaluation of metal zones around the Copper Canyon system was attempted by using metal ratios in production data from the small lode deposits originally used by Roberts and Arnold (1965) to establish the metal zones. Values of Ag/Au ratios in production data from these deposits crudely define a north-south elongate area of reduced Ag/Au ratios, which is underlain largely by feldspathic arenite of the Harmony Formation (**Fig. 14**). In this area, Ag/Au ratios apparently decline to the southeast. Thus, areas southeast of Copper Canyon, which largely are covered by Tertiary and Quaternary gravels, as well as by 3 Ma basalt, may conceal additional Au–mineralized targets.

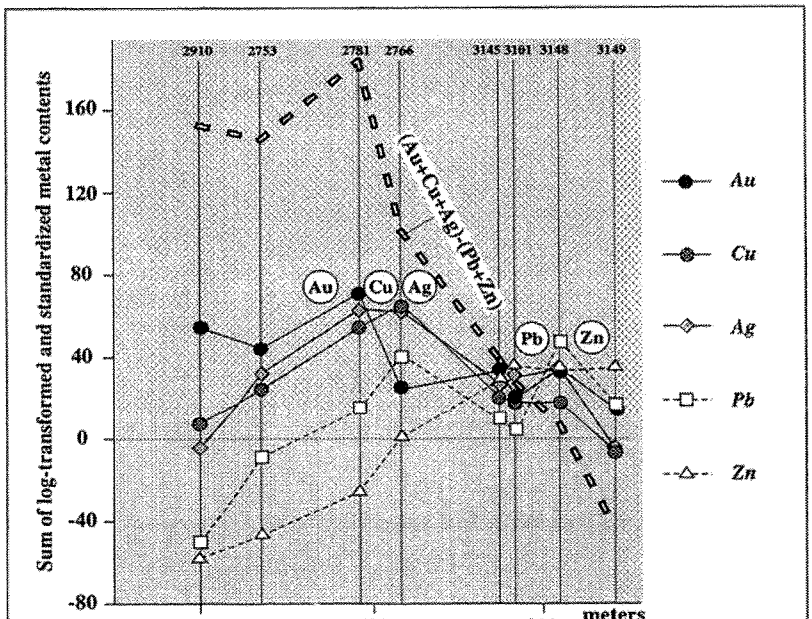

DDH	Metal association
2910	Au—Cu—Ag—Pb—Zn
2753	Au—Ag—Cu—Pb—Zn
2781	Au—Ag—Cu—Pb—Zn
2766	(Cu—Ag)—Pb—Au—Zn

DDH	Metal association
3145	(Au—Zn—Ag)—Cu—Pb
3101	Zu—Ag—(Au—Cu)—Pb
3148	Pb—(Zn—Ag—Au)—Cu
3149	Zn—(Pb—Au)—(Ag—Cu)

Figure 11: Log transformed and standardized metal values summed across mineralized intervals and value of (Au+Cu+Ag)-(Pb+Zn) in selected drill holes along section AA'. Metals listed for drill holes in declining order of standardized metal values. Elements enclosed in parentheses have numerically similar values. Diamond drill hole (DDH) numbers and section AA' same as **Figure 6**.

CLASSIFICATION OF FORTITUDE USING METAL RATIOS

Numerous attempts have been made to use metal ratios to distinguish Au, Cu, and Fe skarns—including Cu/Ag versus Cu/Au (Ettlinger and Ray 1989; Ray and Webster 1990; Ray *et al.,* 1990; Ray and Webster 1995). According to some of these reports, many Au skarns may be characterized by Cu/Au ratios less than 1000. Ray and Webster (1995) further attempted to discriminate Au skarns from other skarns on the basis of plots of log (Au, in ppb) versus log (Cu/Au) in mineralized rocks from a skarn environment, whereas Theodore *et al.* (1991) suggested that all skarns mined primarily for their Au contents should be considered Au skarns (*cf.* Einaudi *et al.,* 1981). Nonetheless, an inherent weakness of the latter classification scheme is that grade and tonnage of a mineralized skarn deposit would have to be known before one could classify it properly. In addition, changing market conditions could result in a predominantly base-metal skarn with byproduct Au evolving into a predominantly Au skarn late in its production history on the basis of fluctuating metal prices (Ray and Webster 1990). If Fortitude Au skarn had been discovered in the 1930s, for example, its high grade Cu–Au–Ag pockets probably would have been mined mostly for their Cu content (roughly 0.2 wt.% Cu overall in the entire deposit, Doebrich *et al.,* 1996), because of the relatively depressed price for Au and the absence of advanced extractive techniques for Au at that time. Some areas within Fortitude attain grades as high as 1 wt.% Cu.

Nonetheless, mineralized samples from five representative drill holes in and around the Fortitude Au skarn were plotted for comparative purposes on a log Au (in ppb) versus log (Cu/Au) diagram, which also includes the Au skarn and other skarn fields of Ray and Webster (1995) (**Fig. 15**). Locations of the five holes are shown on **Figure 6**. Many samples have Cu/Au ratios greater than 1000 and many analyzed samples from only two of the holes (DDHs 2910 and 3101, **Fig. 15**) plot largely in the Au skarn field. Most samples from the five holes plot in the field of Ray and Webster (1995) for other skarns. However, the extremely wide range of Cu–Au correlation coefficients in these mineralized rocks (see above) demonstrates the significant problems involving Cu/Au ratios as discriminants for classification of mineralized skarn at Fortitude. Thus, Cu/Au ratios generally should not be used as indicators for presence of Au skarn without first establishing how Cu–Au correlation coefficients vary spatially. Nonetheless, Myers (1994) found a relatively large volume of mineralized rock in the general area of Fortitude to be characterized by 1000(Au)/Cu >3. This volume of rock mostly encompasses that part of the Fortitude where Cu–Au correlations are strongly positive. Perhaps, these plots (**Fig. 15**) also emphasize the dual classification possibilities for Fortitude: namely, a Cu skarn containing relatively high contents of Au. High Au in the deposit may reflect emplacement of the middle Tertiary skarnrelated, porphyry Cu system at Copper Canyon temporally close to initial breakup of the crust in the Great Basin in this part of Nevada. This time period appears to have been contemporaneous with regionally enhanced introduction of Au on a provincial scale (Seedorff 1991). Further, these data from Fortitude emphasize the difficulty of classifying mineralized skarns on the basis of their precious metal contents (*cf.* Ray and Webster 1990).

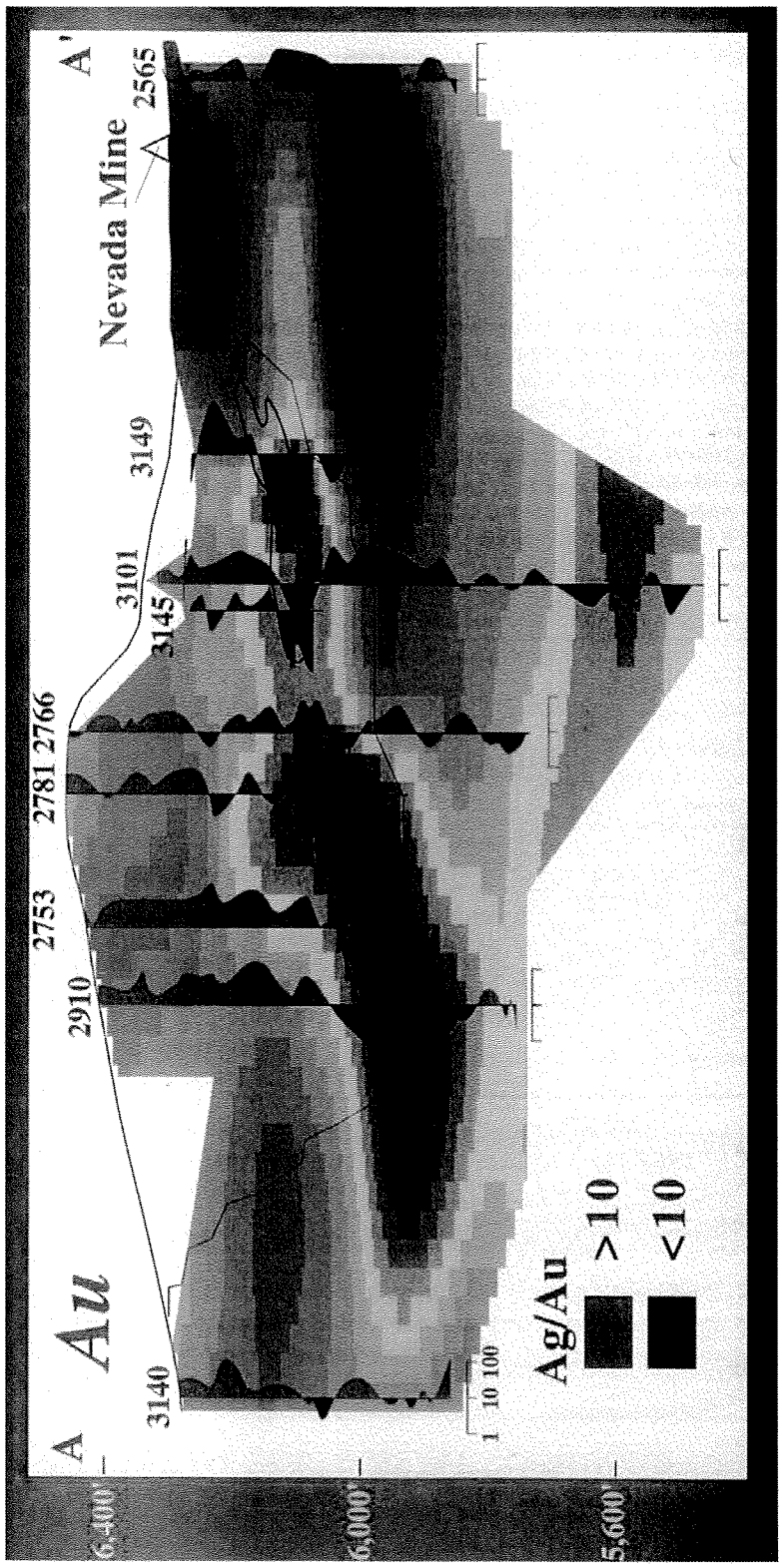

Figure 12: Approximate distributions of Ag/Au ratios in selected diamond drill holes along profile A-A'. Normalized, gridded, and filtered distribution of Au (from **Fig. 6**), as well as projected outline of Lower Fortitude orebodies in profile also shown. "Hotter" intensity of colors indicate higher concentration of Au. Diamond drill hole numbers and profile A-A' same as **Figure 6**.

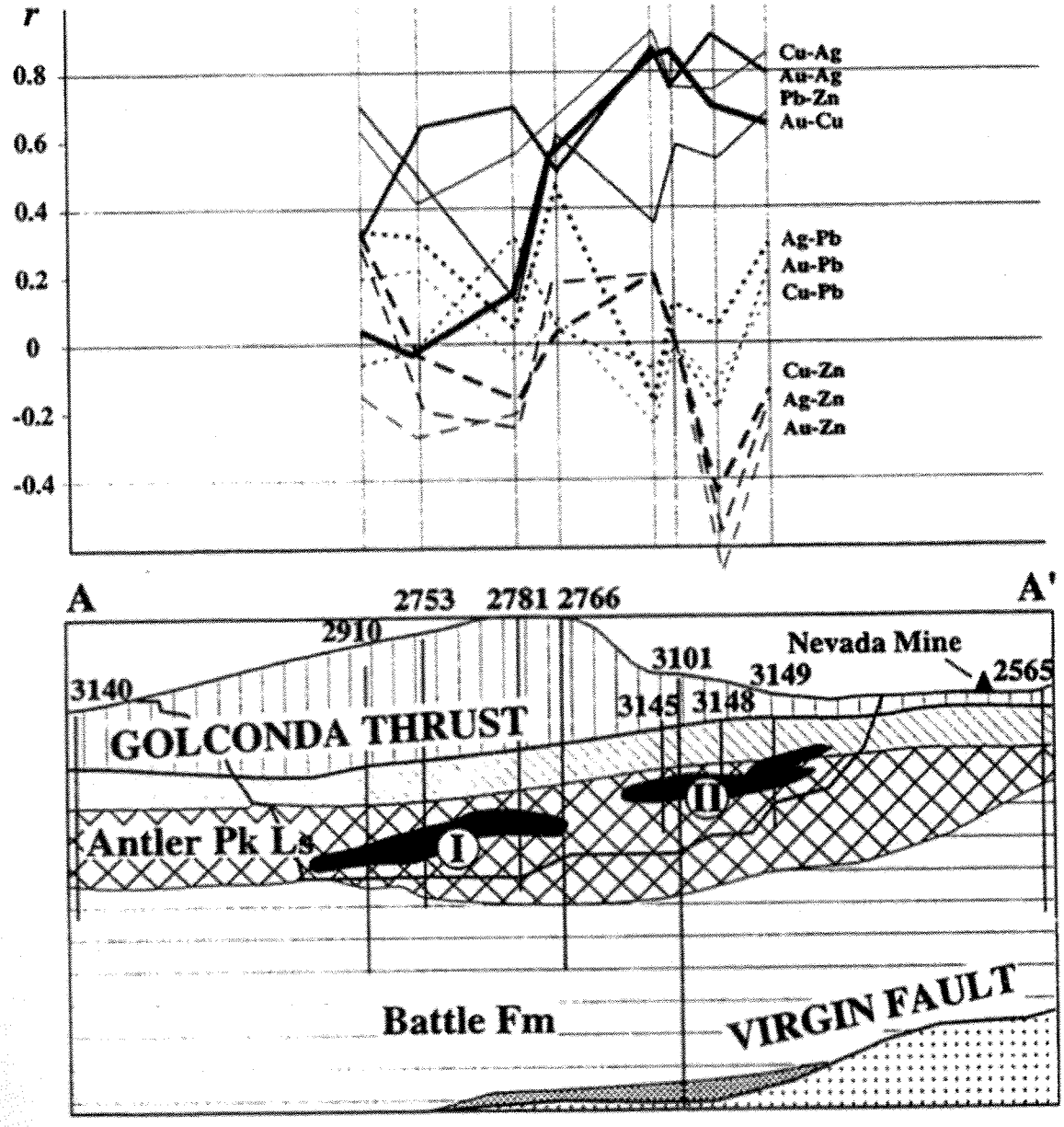

Figure 13: Paired correlation coefficients (r) of proximal (Au, Cu, Ag) and distal (Pb, Zn) elements in eight drill holes along section A A', (Fig. 6). Drill hole numbers same as Figures 8, 11, and 12. Black, projection of Lower Fortitude orebodies (I, Southern orebody; II, Northern orebody) to plane of profile. Geology same as Figure 8A.

DISTRICT-SCALE vs. DEPOSIT-SCALE METAL ZONATIONS

Metal zonations at Copper Canyon vary according to scale. Roberts and Arnold (1965) established that patterns of mining district-scale metal zonation are centered at Copper Canyon and Copper Basin on the basis of a broad distribution of polymetallic veins that had varying amounts of metal production (**Fig. 14**). Roberts and Arnold (1965) classified these polymetallic veins according to the dominant metal produced. However, the large stockwork Mo system at Buckingham (**Fig. 1**), containing resources of as much as 1.4 billion tons at 0.05 wt.% Mo, was not recognized at that time (Loucks and Johnson 1992; Theodore *et al.*, 1992).

Our evaluation revealed concentration of Au and Cu in the proximal parts of the system, as well as the presence of relatively steep declining concentration gradients of these metals northward at the pyritic halo that surrounds the Copper Canyon system (**Fig. 14**). Silver has a more diffuse pattern than Cu and Au, and is somewhat elongate in a north-south direction, straddling the pyritic halo. The bulk of the Pb and Zn are outside the pyritic halo, although substantial concentrations of Pb and Zn are present near the Copper Canyon Cu–Pb–Zn underground mine (deposit no. 11, **Fig. 14**). These elevated contents of Pb and Zn might represent the leading edge of mineralized rock centered at the Midas deposit (deposit no. 10, **Fig. 14**). Reversal of the district-wide metal zoning pattern at the Tomboy-Minnie deposits (deposit nos. 8, 9; **Fig. 15**) (Theodore *et al.*, 1986) also might be a reflection of a focus of fluid influx at the Midas deposit into the Copper Canyon system as the system evolved.

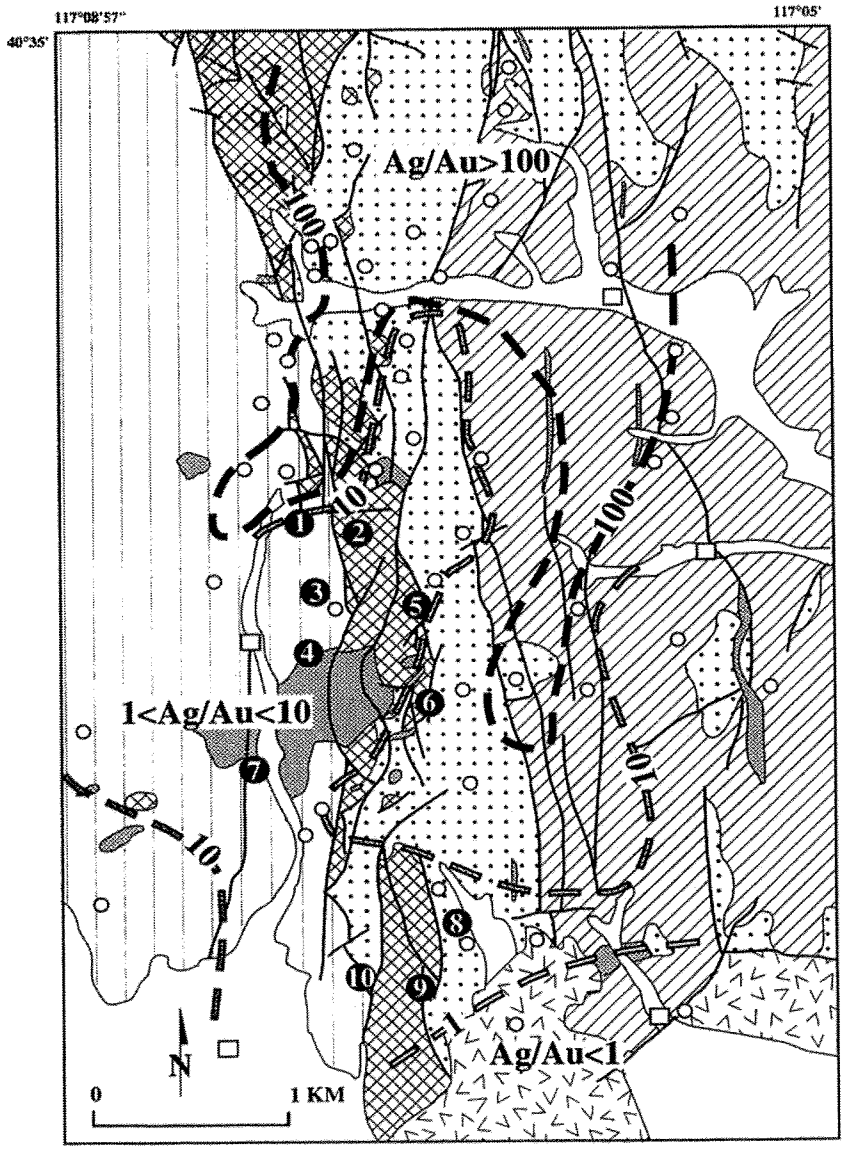

Figure 14: Contoured Ag/Au ratios of production data in polymetallic vein lode deposits in Copper Canyon area, Nevada. Geologic explanation same as Figure 2. Open circles, location of polymetallic vein and placer deposits used to calculate Ag/Au ratios: open squares, placer Au deposits; numbered localities, large Au-Ag deposits, deposit numbers same as Figure 2. Geology modified from Roberts (1964).

Indeed, at a much larger scale, district-wide geochemical patterns are confined tightly around Fortitude Au skarn as well as at some of the other Au skarn deposits (for example, Tomboy-Minnie deposits); Fortitude is close to the transition between Cu–Au–Ag and Pb–Zn zones (**Fig. 8**). District-scale metal zones are similar spatially to those at Bingham Canyon, Utah, except that at Bingham Canyon production from all metal zones has been significantly larger than at Copper Canyon (Einaudi 1982). Further evaluation of metal zones around the Copper Canyon system was attempted by using metal ratios in production data from the small lode deposits originally used by Roberts and Arnold (1965) to establish the metal zones. Values of Ag/Au ratios in production data from these deposits crudely define a north-south elongate area of reduced Ag/Au ratios, which is underlain largely by feldspathic arenite of the Harmony Formation (**Fig. 14**). In this area, Ag/Au ratios apparently decline to the southeast. Thus, areas southeast of Copper Canyon, which largely are covered by Tertiary and Quaternary gravels, as well as by 3 Ma basalt, may conceal additional Au–mineralized targets.

CLASSIFICATION OF FORTITUDE USING METAL RATIOS

Numerous attempts have been made to use metal ratios to distinguish Au, Cu, and Fe skarns—including Cu/Ag versus Cu/Au (Ettlinger and Ray 1989; Ray and Webster 1990; Ray *et al.,* 1990; Ray and Webster 1995). According to some of these reports, many Au skarns may be characterized by Cu/Au ratios less than 1000. Ray and Webster (1995) further attempted to discriminate Au skarns from other skarns on the basis of plots of log (Au, in ppb) versus log (Cu/Au) in mineralized rocks from a skarn environment, whereas Theodore *et al.* (1991) suggested that all skarns mined primarily for their Au contents should be considered Au skarns (*cf.* Einaudi *et al.,* 1981). Nonetheless, an inherent weakness of the latter classification scheme is that grade and tonnage of a mineralized skarn deposit would have to be known before one could classify it properly. In addition, changing market conditions could result in a predominantly base-metal skarn with byproduct Au evolving into a predominantly Au skarn late in its production history on the basis of fluctuating metal prices (Ray and Webster 1990). If Fortitude Au skarn had been discovered in the 1930s, for example, its high grade Cu–Au–Ag pockets probably would have been mined mostly for their Cu content (roughly 0.2 wt.% Cu overall in the entire deposit, Doebrich *et al.,* 1996), because of the relatively depressed price for Au and the absence of advanced extractive techniques for Au at that time. Some areas within Fortitude attain grades as high as 1 wt.% Cu.

Nonetheless, mineralized samples from five representative drill holes in and around the Fortitude Au skarn were plotted for comparative purposes on a log Au (in ppb) versus log (Cu/Au) diagram, which also includes the Au skarn and other skarn fields of Ray and Webster (1995) (**Fig. 15**). Locations of the five holes are shown on **Figure 6**. Many samples have Cu/Au ratios greater than 1000 and many analyzed samples from only two of the holes (DDHs 2910 and 3101, **Fig. 15**) plot largely in the Au skarn field. Most samples from the five holes plot in the field of Ray and Webster (1995) for other skarns. However, the extremely wide range of Cu–Au correlation coefficients in these mineralized rocks (see above) demonstrates the significant problems involving Cu/Au ratios as discriminants for classification of mineralized skarn at Fortitude. Thus, Cu/Au ratios generally should not be used as indicators for presence of Au skarn without first establishing how Cu–Au correlation coefficients vary spatially. Nonetheless, Myers (1994) found a relatively large volume of mineralized rock in the general area of Fortitude to be characterized by 1000(Au)/Cu >3. This volume of rock mostly encompasses that part of the Fortitude where Cu–Au correlations are strongly positive. Perhaps, these plots (**Fig. 15**) also emphasize the dual classification possibilities for Fortitude: namely, a Cu skarn containing relatively high contents of Au. High Au in the deposit may reflect emplacement of the middle Tertiary skarnrelated, porphyry Cu system at Copper Canyon temporally close to initial breakup of the crust in the Great Basin in this part of Nevada. This time period appears to have been contemporaneous with regionally enhanced introduction of Au on a provincial scale (Seedorff

1991). Further, these data from Fortitude emphasize the difficulty of classifying mineralized skarns on the basis of their precious metal contents (*cf.* Ray and Webster 1990).

DISCUSSION AND CONCLUSIONS

Zoned metal relations between Cu (proximal) and Pb and Zn (distal) are similar to metal distributions that one would infer from the experimental solubility studies of Hemley *et al.* (1992). Hemley *et al.* (1992) showed, for example, solubilities for Cu, Pb, and Zn are 40 ppm, 613 ppm, and 423 ppm, respectively, in a system under the following conditions: (1) pH buffered by K–feldspar, muscovite, and quartz; (2) 1 *m* total Cl–, (3) 400°C and 100 MPa total pressure; and (4) containing the assemblage pyrite, pyrrhotite, magnetite, sphalerite, galena, and chalcopyrite. These P–T–X conditions, with the exception of pressure, probably are close to those prevailing at the time of circulation of much of the ore-forming fluids in the environment of Fortitude. Pressures at the time of mineralization probably were about 40 MPa (Myers 1994). The much higher experimentally determined solubilities of Pb and Zn than Cu suggests that Pb and Zn should remain in solution longer than Cu and that they would inevitably be carried in mineralizing, magma-derived fluids down any existing pressure-temperature gradient toward distal parts of the orebody. Nonetheless, decreasing temperature and oxygen fugacity, increasing pH, as well as boiling probably all contribute significantly to eventual deposition of metals (*cf.* Seward 1989). Separation of Pb and Zn loci from each other at Fortitude—Zn is more distal (**Fig. 8**)—may result from differences in their metal-complex stabilities (Seward and Barnes 1997). Although significant quantities of Au and Ag can be transported as Au– and Ag–bisulfide complexes and deposited because of pH or redox changes (Shenberger and Barnes 1989; Gammons and Barnes 1989), at Fortitude, where Au is concentrated in the distal parts of the system, activity of aqueous sulfur concentrations may be less important, because fugacity of sulfur may be relatively low because of the presence of pyrrhotite and arsenopyrite. Destabilization of Au–chloride complexes may be more important.

As a further example of the sources of the fluids associated with genesis of the Fortitude and surrounding deposits, 10 percent crystallization of some intermediate composition magmas at pressures of about 50 MPa could result in saturation of magma by H_2O (Meinert 1993; *cf.* Burnham 1979). However, second or resurgent boiling may occur at any point and continue to complete solidification of the magma as the carapace solidifies into the magma. The distribution of metals in multi-leveled horizons near the Fortitude deposit further suggests that several pulses of mineralization—all involving complicated scenarios of retrograde fluid collapse during a protracted late Eocene and (or) early Oligocene hydrothermal event—may have formed the complex orebodies there, and that additional sites of mineralized rock may be present well below the presently known orebodies. Some of these deep targets are currently (1999) being evaluated. The close spatial association between Cu and Au loci of mineralized rock (**Fig. 8**) is compatible with the thermodynamic calculations of Gammons and Williams-Jones (1997) who showed that in a shallow-seated geologic environment magmatic fluids will have a tendency to boil shortly after their exsolution from a magma and that Au in solution will partition into the brine phase generally together with Cu. Heinrich *et al.* (1999) recently have shown that both Cu and Au can be strongly partitioned into the vapor phase, although they further emphasize that many element-fractionating processes likely are to have been operative at various times in large magmatic-hydrothermal systems. Presence of the bulk of the highest grade Au ore near the outer limit of development of skarn in the system may result from a ponding of fluids behind the skarn front wherein destabilization of Au chloride complexes may have occurred as the system declined thermally with time (Gray *et al.*, 1995).

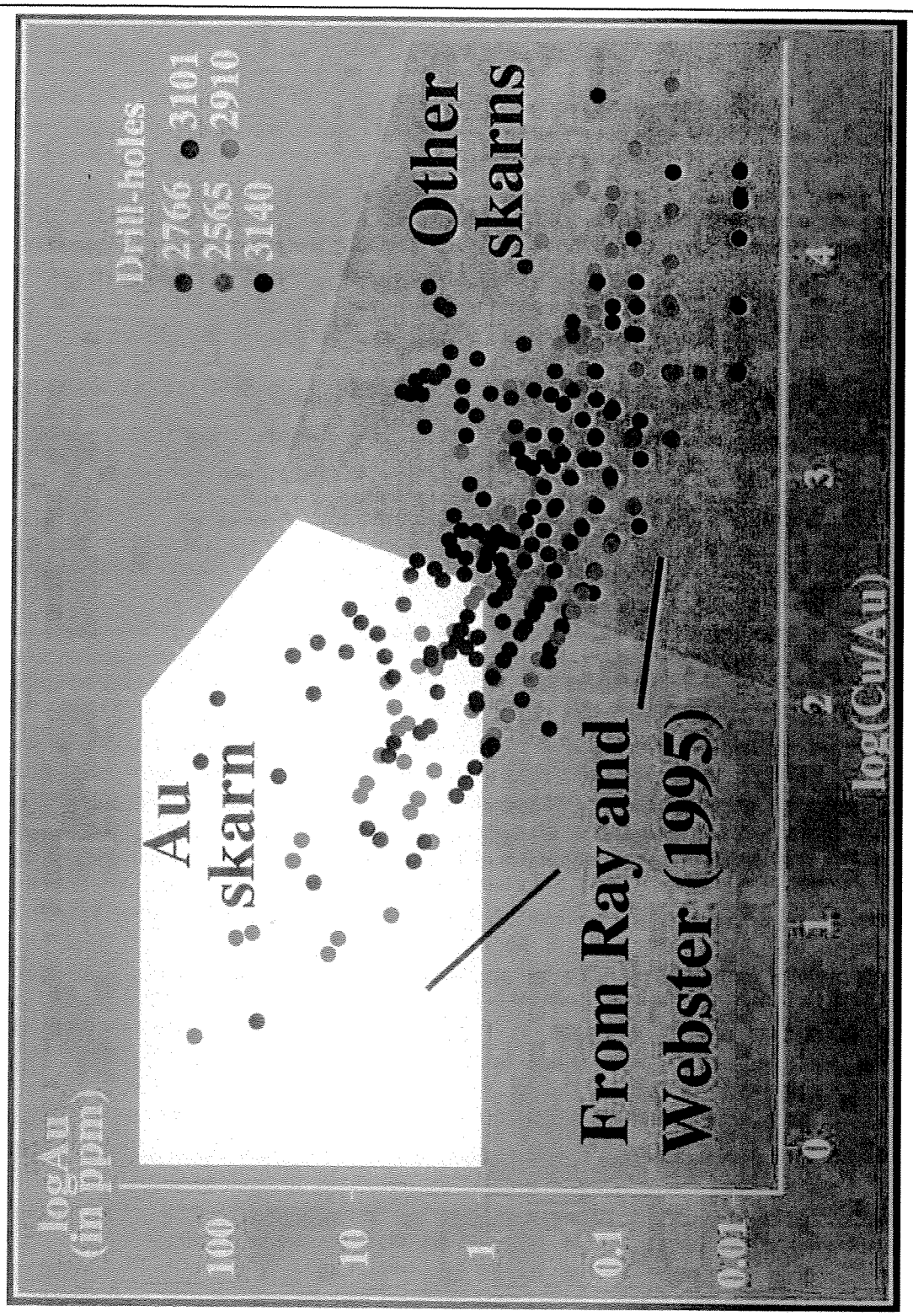

Figure 15: Gold versus Cu/Au ratio in five selected holes along section AA'. Fields for Au skarn and other skarns from Ray and Webster (1995). Drill hole numbers same as Figure 6.

Comparison of the volume of granodioritic rock apparently associated with genesis of the Copper Canyon porphyry system with that documented at other porphyry Cu systems provides additional insight into development of the system at Copper Canyon. The altered granodiorite of Copper Canyon is laccolithic and is characterized by a number of narrow, highly irregular apophyses protruding into its wallrock (Theodore and Blake 1975; Doebrich *et al.,* 1996). Some parts of the body are only 300 m thick, yielding estimates of about 0.4 km3 for the entire body if one assumes a cylindrical shape with a 600–m radius and a generous 370–m deep chamber. Caprock breccia in its center suggests that present exposure levels are near its uppermost levels of emplacement (Theodore and Blake 1975). The 10 large orebodies at Copper Canyon (deposit nos. 1–10, **Fig. 2; Table 1) and the nearby to the west Sunshine deposit comprise approximately 115 million short tons** of ore (**Table 1**), most of which were developed primarily for their commercial Au and Ag contents. If we assume that these 11 orebodies contained, on average, as much as 0.3 wt.% Cu—accurate Cu contents are not available—then the bodies would contain 0.34 million tons Cu. Further, a much larger amount of Cu is present in the laccolith, which has an average grade of approximately 0.2 wt.% Cu (Theodore and Blake 1975). Another point to bear in mind is that all of these Au ore bodies are relatively close to the center of magmatic activity in this part of the mining district.

Many aspects concerning magma volumes associated with generation of porphyry Cu deposits can be ascertained from the Middle Jurassic Yerington, Nev., porphyry Cu system because it has been tilted during Tertiary extension (Dilles and Proffett 1995). At Yerington, relatively small calc-alkaline granite porphyry dikes are associated temporally and genetically with porphyry Cu mineralized rock that developed at paleodepths of about 3–5 km—the dikes evolved from the unexposed Middle Jurassic Luhr Hill Granite of Dilles and Proffett (1995). The latter is estimated to comprise a volume of approximately 65 km^3 (Dilles 1987). The four Cu deposits at Yerington—Yerington, Bear-Lagomarsino, MacArthur, and Ann Mason—most directly associated with this volume of magma contained roughly 5 million tons Cu (Dilles and Proffett 1995). Numerical simulations involving experimental data concerning partitioning of Cu between magma and aqueous fluids at total pressures near those probably prevailing during emplacement of the Copper Canyon system appear to be roughly compatible with these values (Cline and Bodnar 1991). Further, Cline (1995) has shown that, at 50 MPa, 16.5 km3 calc-alkaline magma is necessary to produce approximately 2 million tons Cu. All of the above suggests that it should not be surprising to find another apex for a mineralizing cupola of altered granodiorites at Copper Canyon, because most metal in the deposits at Copper Canyon is likely to have been derived ultimately from a deep magma source much larger than the small exposed laccolithic body (*cf.* Theodore and Blake 1975). If we assume that the same efficiency of Cu extraction versus volume of associated magma at Yerington prevailed at Copper Canyon, then the altered granodiorite of Copper Canyon could have produced at most approximately 0.03 million tons Cu. This is much smaller than our estimate of 0.34 million tons Cu in the 11 major deposits, and the additional large amount of Cu in the altered granodiorite.

We suggest that there may be another apex of a mineralizing cupola of granodiorite somewhere at depth below the general area of the Fortitude deposits, and that this granodiorites may have a series of stacked zones of mineralized rock above it (**Figs. 8, 10, 12**). Feeders for mineralized rock in the Fortitude deposits might be the Copper Canyon and Virgin faults, as well as minor fault splays associated with them. The deepest drill-hole sample along section AA' containing strongly anomalous Au is an altered granodiorite dike (**Fig. 13**), which also contains disseminated pyrite and some pyrite along fractures. This dike intruded near the contact between the Battle and Harmony Formations. If near-surface metal zonation around Lower Fortitude is repeated at depth, then the second locus of Pb concentration well below Fortitude should be succeeded downwards by a nearby Au zone, and by an even deeper Cu zone—possibly in rocks of the Harmony Formation (**Fig. 16**). These vertically stacked mineralized rocks in the distal parts of the Fortitude are compatible with deep feeders inferred to be present in the general area by Myers (1994). The deep Cu could comprise a fracture-controlled, non-

skarn occurrence in altered rocks of the Harmony Formation, similar to that present in some other porphyry systems elsewhere in the mining district (**Fig. 16**). For example, in the Elder Creek porphyry Cu system in the central part of the Battle Mountain Mining District (**Fig. 1**), Gostyayeva *et al.* (1996) report the presence of narrow chalcopyrite-rich intercepts as stockworks in propylitically altered rocks of the Harmony Formation. If it becomes apparent from additional geochemical studies of the Phoenix deposit that it includes a reversal of metal zones (Pb, Cu, Au) towards exposed granodiorite—in other words, a reversal of the alignment of metal zones present in Fortitude—then our preferred placement of the inferred cupola of granodiorites would be approximately equidistant between the Fortitude and Phoenix deposits.

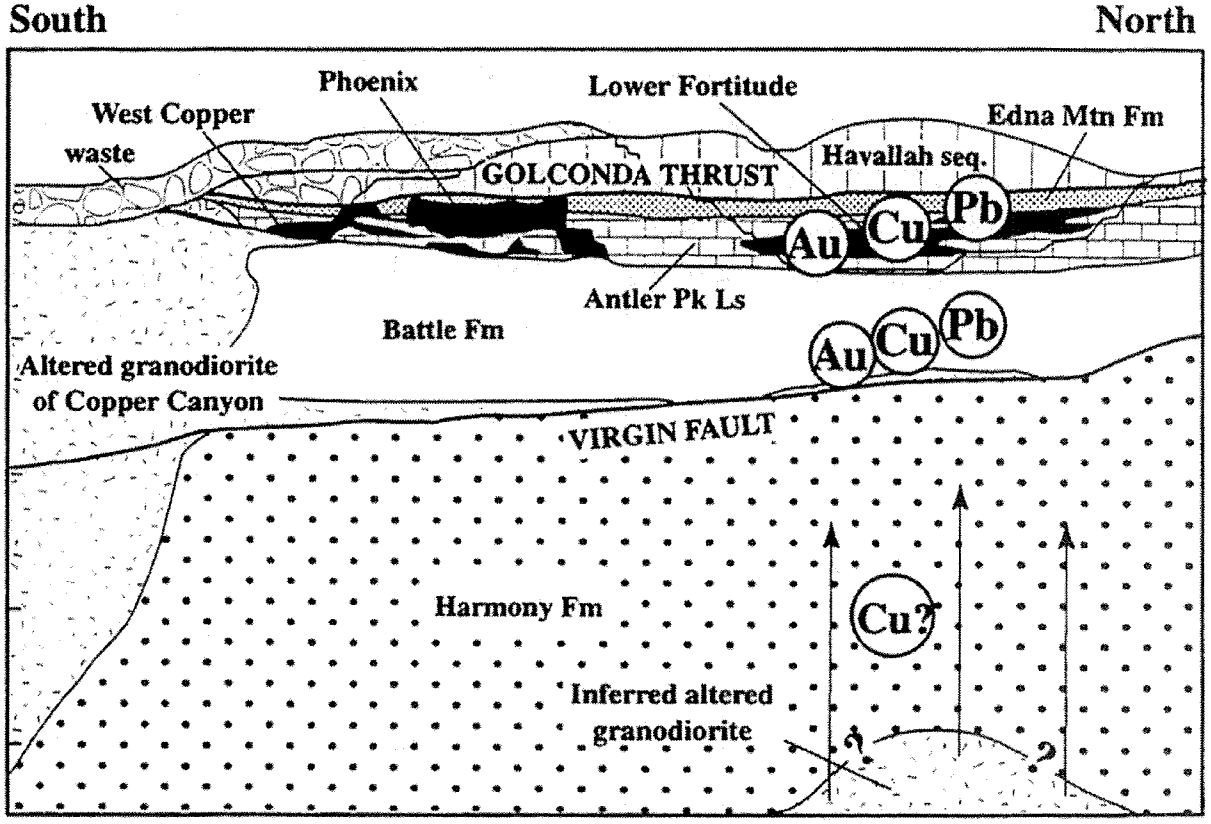

Figure 16: Schematic cross section through Fortitude, Phoenix, and West Copper deposits showing known and inferred (queried) loci of mineralized rock. Filtering and gridding procedures turned out to be an effective tool, in our judgement, to synthesize enormous amounts of geochemical data at Copper Canyon, and to develop a model for prograde fluid flow.

Finally, metal distributions in a porphyry environment must be considered relative to their configurations in three-dimensional space. Presence or absence of metals should be evaluated carefully by considering (1) non-orthogonal prograde fluid paths during metallization; and (2) the potential influence of prograde metal zonations—some quite subtle—from other nearby loci of mineralized rock. Filtering and gridding procedures turned out to be an effective tool, in our judgment, to synthesize enormous amounts of geochemical data at Copper Canyon, and to develop a model of prograde fluid flow.

REFERENCES

Atkinson, W.W., Jr. and Einaudi, M.T. (1978): Skarn formation and mineralization in the contact aureole at Carr Fork, Bingham, Utah. *Econ. Geol.* 73, 1,326–1,365.

Beus, A.A. and Grigorian, S.V. (1977): *Geochemical exploration methods for mineral deposits.* Applied Publishing, Ltd., Wilmette, Illinois.

Blakely, R.J., (1994): *Potential theory in gravity and magnetic applications*. Cambridge University Press, New York.

Briggs, I.C. (1974): Machine contouring using minimum curvature. *Geophysics* 39, 39–48.

Burnham, C.W. (1979): Magmas and hydrothermal fluids. *In Geochemistry of Hydrothermal Ore Deposits, Second edition* (H.L. Barnes, ed.), John Wiley and Sons, Inc., 71–136.

Cabri, L.J., Chryssoulis, S.L., De Villiers, J.P.R., Laflamme, J.H.G. and Buseck, P.R. (1989): The nature of "invisible" gold in arsenopyrite. *Can. Mineral.* 27, 353–362.

Casquet, C. and Tornos, F. (1991): Influence of depth and igneous chemistry on ore development in skarns. The Hercynian belt of the Iberian peninsula. *In Skarns—their genesis and metallogeny* (A.M. Aksyuk, A.M., *et al.*, eds.), Theophrastus Publications S.A., Athens, 555–591.

Chaffee, M.A. (1982): A geochemical study of the Kalamazoo porphyry copper deposit. *In Advances in geology of the porphyry copper deposits* (S.R. Titley, ed.), Univ. Arizona Press, Tucson, 211–225.

Cline, J.S. (1995): Genesis of porphyry copper deposits: The behavior of water, chloride, and copper in crystallizing melts. *In Porphyry copper deposits of the American Cordillera* (F.W. Pierce and J.G. Bolm, eds.), *Ariz. Geol. Soc. Digest* 20, 69–82.

Cline, J.S. and Bodnar, R.J. (1991): Can economic porphyry copper mineralization be generated by a typical calc-alkaline melt? *J. Geophys. Res.* 96, B5, 8,113–8,126.

Cox, D.P. and Singer, D.A. (1992): Grade and tonnage model of distal disseminated Ag–Au. *In Developments in Mineral Deposit Modeling* (J.D. Bliss, ed.), *U.S. Geol. Survey Bull.* 2004.

Dilles, J.H. (1987): Petrology of the Yerington Batholith: Evidence for evolution of porphyry copper ore fluids. *Econ. Geol.* 82, 1,750–1,789.

Dilles, J.H. and Proffett, J.M. (1995): Metallogenesis of the Yerington batholith, Nevada. *In Porphyry Copper Deposits of the American Cordillera* (F.W. Pierce and J.G. Bolm, eds.), *Ariz.Geol. Soc. Digest* 20, 306–315.

Doebrich, J.L. (1995): Geology and mineral deposits of the Antler Peak 7.5–minute quadrangle, Lander County, Nevada. *Nev. Bur. Mines Geol. Bull.* 109.

Doebrich, J.L. and Theodore, T.G. (1996): Geologic history of the Battle Mountain Mining District, Nevada, and regional controls on the distribution of mineral systems. *In Geology and Ore Deposits of the American Cordillera* (A.R. Coyner and P.L. Fahey, eds.), *Geol. Soc. Nevada Symposium Proceedings* 1, 453–483.

Doebrich, J.L., Wotruba, P.R., Theodore, T.G., Mcgibbon, D.H. and Felder, R.P. (1996): Field trip guidebook for Trip H—Geology and ore deposits of the Battle Mountain Mining District. *In Field Trip Guidebook Compendium* (S.M. Green and Eric Struhsacker, eds.), *Geol. Soc. Nevada*, Reno, 327–388.

Einaudi, M.T. (1982): Description of skarns associated with porphyry copper plutons, southwest North America. *In Advances in Geology of the Porphyry Copper Deposits* (S.R. Titley, ed.), Univ. Arizona Press, Tucson, 139–183.

Einaudi, M.T. (1990): Zoning of gold and silver in central portions of porphyry copper districts [abs.]. *In Geology and Ore Deposits of the Great Basin* (Bob Cuffney, ed.), *Geol. Soc. Nevada, Program with Abstracts*, Reno, 59–60.

Einaudi, M.T., Meinert, L.D. and Newberry, R.J. (1981): Skarn deposits. *In Seventy-fifth Anniversary Volume*, 1905–1980 (B.J. Skinner, ed.), Econ. Geol. Pub. Co., New Haven, 317–391.

Ettlinger, A.D. (1990): A geological analysis of gold skarns and precious-metal enriched iron and copper skarns in British Columbia, Canada. Ph.D. thesis, Washington State Univ., Pullman, Geological Society of Nevada Fall 1999 Field Trip Guidebook

Ettlinger, A.D., Meinert, L.D. and Ray, G.E. (1992): Gold skarn mineralization and fluid evolution in the Nickel Plate deposit, Hedley District, British Columbia. *Econ. Geol.* 87, 1541–1565.

Ettlinger, A.D. and Ray, G.E. (1989): Precious metal enriched skarns in British Columbia: An overview and geological study. *British Col. Min. Energy, Mines & Petrol. Resources Paper* 1989–3.

Fonteilles, M., Soler, P., Demange, M., Derre, C., Krier-Schellen, A.D., Verkaeren, J., Guy, B. and Zahm, A. (1989): The scheelite skarn deposit of Salau (Ariege, French Pyrenees). *Econ. Geol.* 84, 1172–1209.

Gammons, C.H. and Barnes, H.L. (1989): The solubility of Ag2S in near-neutral aqueous sulfide solutions at 25 to 300°C. *Geochim. et Cosmochim. Acta* 53, 279–290.

Gammons, C.H. and Williams-Jones, A.E. (1995): The solubility of Au–Ag alloy + AgCl in HCl/NaCl solutions at 300°C: New data on the solubility of Au(I) chloride complexes in hydrothermal fluids. *Geochim. et Cosmochim. Acta* 59, 3453–3468.

Gammons, C.H. and Williams-Jones, A.E. (1997): Chemical mobility of gold in the porphyryepithermal environment. *Econ. Geol.* 92, 45–59.

Gostyayeva, N., Theodore, T.G. and Lowenstern, J.B. (1996): Implications of fluid-inclusion relations in the Elder Creek porphyry copper system, Battle Mountain Mining District, Nevada. *U.S. Geol. Survey Open-File Rept.* 96–268.

Gray, N., Mandyczewsky, A. and Hine, R. (1995): Geology of the zoned gold skarn system at Junction Reefs, New South Wales. *Econ. Geol.* 90, 1533–1552.

Grimes, D.J. and Marranzino, A.P. (1968): Direct-current arc and alternating-current spark emission spectrographic field methods for the semiquantative analysis of geologic materials. *U.S. Geol .Survey Circ.* 591.

Guy, B. (1979): Petrology and isotope geochemistry at the scheelitw-bearing skarns at Costabonne, eastern Pyrenees, France. Ph.D. thesis, L'Ecole Nat'l Superieure Mines, Paris.

Haffty, J., Riley, L.B. and Goss, W.D. (1977): A manual on fire assaying and determination of the noble metals in geological materials. *U.S. Geol. Survey Bull.* 1443.

Harris, D.C. (1990): The mineralogy of gold and its relevance to gold recoveries. *Mineral. Deposita* 25, S3–S7.

Heinrich, C.A., Gunther, D., Audetat, A., Ulrich, T. and Frischnecht (1999): Metal fractionation between magmatic brine and vapor, determined by microanalysis of fluid inclusions. *Geology* 27, 755–758.

Hemley, J.J., Cygan, G.L., Fein, J.B., Robinson, G.R. and D'Angelo, W.M. (1992): Hydrothermal ore-forming processes in the light of studies in rock-buffered systems: I. Iron-copper-zinc-lead sulfide solubility relations. *Econ. Geol.* 87, 1–22.

Ivosevic, S.W. and Theodore, T.G. (1996): Weakly developed porphyry system at upper Paiute Canyon, Battle Mountain Mining District, Nevada. *In Geology and Ore Deposits of the American Cordillera, Symposium Proceedings* (A.R. Coyner and P.L. Fahey, eds.), *Geol. Soc. of Nevada* 3, 1573–1594.

Johnson, T.W. (1991): Geology, hydrothermal alteration, and Cu–Au–Ag skarn and replacement mineralization in the northern part of the New World district, Park County, Montana. M.S. thesis, Washington State Univ., Pullman, Washington.

Johnson, T.W. (1992): Geology and paragenesis of the McLaren copper-silver-gold skarn and replacement deposit, New World District, Park County, Montana [abs.]. *In Guidebook for the Red Lodge-Beartooth Mountains-Stillwater Area* (J.E. Elliott, ed.), *Northwest Geology* 20–21, 61–62.

Johnson, T.W. and Meinert, L.D. (1994): Au–Cu–Ag skarn and replacement mineralization in the McLaren deposit, New World District, Park County, Montana. *Econ. Geol.* 89, 969–993.

Korobeinikov, A.F. (1991): Gold conduct in the contact-metasomatic processes of intrusions. *In Skarns—Their Genesis and Metallogeny* (A.M. Aksyuk, *et al.*, eds.), Theophrastus Publications S.A., Athens, 203–226.

Kotlyar, B.B., Theodore, T.G. and Jachens, R.C. (1995): Re-examination of rock geochemistry in the Copper Canyon area, Lander County, Nevada. *U.S. Geol. Survey Open-File Report* 95–816.

Loucks, T.A. and Johnson, C.A. (1992): Economic geology. *In* T.G. Theodore, D.W. Blake, T.A. Loucks and C.A. Johnson, Geology of the Buckingham stockwork molybdenum deposit and surrounding area, Lander County, Nevada. *U.S. Geol. Survey Prof. Paper* 798–D, *D*101–*D*138.

Masters, T. (1993): Practical neural network recipes in C++. Academic Press, San Diego, California.

Mckee, E.H. (1992): Potassium argon and 40Ar/39Ar geochronology of selected plutons in the Buckingham area. *In* T.G. Theodore, D.W. Blake, T.A. Loucks and C.A. Johnson, Geology of the

Buckingham stockwork molybdenum deposit and surrounding area, Lander County, Nevada. *U.S. Geol. Survey Prof. Paper* 798–D, *D*36–*D*40.

Meinert, L.D. (1987): Skarn zonation and fluid evolution in the Groundhog Mine, Central Mining District, New Mexico. *Econ. Geol.* 82, 523–545.

Meinert, L.D. (1989): Gold skarn deposits—geology and exploration criteria. *In The Geology of Gold Deposits, the Perspective in 1988* (R.R. Keays, W.R.H. Ramsay and D.I. Groves, eds.) *Econ. Geol., Monograph* 6, 537–552.

Meinert, L.D. (1993): Igneous petrogenesis and skarn deposits. *In Mineral Deposit Modeling* (R.V. Kirkham, W.D. Sinclair, R.I. Thorpe and J.M. Duke, eds.), *Geol. Assoc. Canada Spec. Paper* 40, 569–583.

Meinert, L.D. (1998): A review of skarns that contain gold. *In Mineralized Intrusion-related Skarn Systems* (D.R. Lentz, ed.*), Mineral. Assoc. Can. Short Course* 26, 359–414.

Meinert, L.D., Hefton, K.K., Mayes, David and Tasiran, Ian (1997): Geology, zonation, and fluid evolution of the Big Gossan Cu–Au skarn deposit, Ertsberg District. *Econ. Geol.* 92, 509–534.

Mueller, A.G. (1997): The Nevoria gold skarn deposit in Archean iron formation, Southern Cross Greenstone Belt, western Australia: I. Tectonic setting, petrography, and classification. *Econ. Geo.* 92, 181–209.

Murchey, B.L. (1990): Age and depositional setting of siliceous sediments in the upper Paleozoic Havallah sequence near Battle Mountain, Nevada: Implications for the paleogeography and structural evolution of the western margin of North America. *In Paleozoic and Early Mesozoic Paleogeographic Relations; Sierra Nevada, Klamath Mountains,and Related Terranes* (D.S. Harwood and M.M. Miller, eds.), *Geol. Soc. America Spec. Paper* 255, 137–155.

Myers, G.L. (1994): Geology of the Copper Canyon-Fortitude skarn system, Battle Mountain, Nevada. Ph.D. thesis, Washington State Univ., Pullman, Washington.

Nash, J. T. and Theodore, T.G. (1971): Ore fluids in a porphyry copper deposit at Copper Canyon, Nevada. *Econ. Geol.* 66, 385–399.

Ray, G.E. and Dawson, G.L. (1994): The geology and mineral deposits of the Hedley gold skarn district, southern British Columbia. *British Col. Min. Energy, Mines & Petrol. Resources Bull.* 87.

Ray, G.E., Dawson, G.L and Simpson, R. (1988): Geology, geochemistry, and metallogenic zoning in the Hedley gold-skarn camp. *British Col. Min. Energy, Mines & Petrol. Resources*, Geol. Fieldwk. 1988–1, 59–80.

Ray, G.E., Ettlinger, A.D. and Meinert, L.D. (1990): Gold skarns: Their distribution, characteristics, and problems in classification. *British Col. Min. Energy, Mines & Petrol. Resources*, Geol. Fieldwk. 1990–1, 237–246.

Ray, G.E. and Webster, I.C.L. (1990): An overview of skarn deposits. *In Ore Deposits, Tectonics, and Metallogeny in the Canadian Cordillera* (W.J. McMillan *et al.*, eds.). *Geol. Assoc. Canada*, Short Course Notes, 7–1 to 7–55.

Ray, G.E. and Webster, I.C.L. (1995, The geochemistry of mineralized skarns in British Columbia. *British Col. Min. Energy, Mines & Petrol. Resources* 1995–1, 371–383.

Roberts, R.J. (1964): Stratigraphy and structure of the Antler Peak quadrangle, Humboldt and Lander Counties, Nevada. *U.S. Geol. Survey Prof. Paper* 459–A.

Roberts, R.J. and Arnold, D.C. (1965): Ore deposits of the Antler Peak quadrangle, Humboldt and Lander Counties, Nevada. *U.S. Geol. Survey Prof.Paper* 459–B.

Roberts, R.J., Hotz, P.E., Gilluly, J. and Ferguson, H.G. (1958): Paleozoic rocks in north-central Nevada. *Am. Assoc. Petrol. Geol. Bull.* 42, 2813-2857.

Seedorff, E. (1991): Magmatism, extension, and ore deposits of the Eocene to Holocene age in the Great Basin – mutual effects and preliminary proposed genetic relationships. *In Geology and Ore Deposits of the Great Basin, Symposium Proceedings* (Raines, G.L., R.E. Lisle, R.W. Schafer and W.H. Wilkinson, eds.), *Geol Soc. Nevada,* Reno, 133-178.

Seward, T.M. (1989): The hydrothermal chemistry of gold and its implications for ore formation: Boiling and conductive cooling as examples, *In The Geology of Ore Deposits: The Perspective in 1988* (R.R. Keays, W.R.H. Ramsay and D.I. Groves, eds.) *Econ. Geol. Monograph* 6, 398-404.

Seward, T.M. and Barnes, H.L. (1997): Metal transport by hydrothermal fluids. *In Geochemistry of Hydrothermal Ore Deposits, Third Edition* (H.L. Barnes, ed.) John Wiley and Sons, Inc., New York, 435-486.

Shenberber, D.M. and Barnes, H.L. (1989): Solubility of gold in aqueous sulfide solutions from 150 to 350 °C. *Geochim. et Cosmochim.* Acta 53, 269-278.

Siberling, N.J. and Roberts, R.L. (1962): Pre-Tertiary stratigraphy and structure of northwestern Nevada. *Geol. Soc. America Special Paper 71.*

Soler, P. (1980): Gologie du gisement de Salau. *Bur. Recherches Geol. Min. Mem.* 99, 205-216.

Steward, J.H. and Mckee, E.H. (1977): Geology and mineral deposits of Lander County, Nevada: Part I, geology. *Nev. Bur. Mines and Geol. Bull. 88.*

Theodore, T.G. (1969): Surface distribution of selected elements around the Copper Canyon copper-gold-silver open pit mine, Lander County, Nevada. *U.S. Geol. Survey Open-File Report* 69-278.

Theodore, T.G. (1970): Rock analyses around the Copper Canyon open pit mine, Lander County, Nevada. *U.S. Geol. Survey Open-File Report* 70-325.

Theodore, T.G. (1991): Preliminary geology map of the Valmy quadrangle, Humboldt County, Nevada. *U.S. Geol. Survey Open-File Report* 91-430.

Theodore, T.G. (1996): Geology and implications of silver/gold ratios of the Elder Creek porphyry copper system, Battle Mountain Mining District, Nevada. *In Geology and Ore Deposits of the American Cordillera, Symposium Proceedings* (Coyner, A.R. and Fahey, P.L., eds.), *Geol. Soc. Nevada,* Reno, 1557-1571.

Theodore, T.G. (1999): Implications of regional geology and geochemistry in the northern Carlin trend, southern Tuscarora Mountains, Nevada [Extended abs.]. *Ralph J. Roberts Sixth Distinguished Lecture in Economic Geology, Program, Mackay School of Mines*, Reno.

Theodore, T.G. and Blake, D.W. (1975): Geology and geochemistry of the Copper Canyon porphyry copper deposit and surrounding area, Lander County, Nevada. *U.S. Geol. Survey Prof. Paper* 798-B.

Theodore, T.G. and Blake, D.W. (1978): Geology and geochemistry of the West ore body and associated skarns, Copper Canyon porphyry copper deposits, Lander County, Nevada. *U.S. Geol. Survey Prof. Paper* 798-C.

Theodore, T.G. and Hammarstrom J.M. (1991): Petrochemistry and fluid-inclusion study of skarns from the northern Battle Mountain mining district, Nevada. *In Skarns – Their Genesis and Metallogeny* (Aksyuk et al., eds.), Theophrastus Publications S.A., Athens, 497-554.

Theodore, T.G. and Nash J.T. (1973): Geochemical and fluid zonation at Copper Canyon, Lander County, Nevada. *Econ. Geology* 68, 565-570.

Theodore, T.G., Hammarstrom, J.M. and Bliss, J.D. (1991): Gold-bearing skarns. *U.S. Geol. Survey Bulletin* 1930.

Wilson, S.A., Kane, J.S., Crock, J.G. and Hatfield, D.B. (1987): Chemical methods of separation for optical emission, atomic absorption spectrometry, and colorimetry. *In Methods for Geochemical Analysis (P.A. Baedecker ed.), U.S. Geol. Survey Bulletin* 1770, D1-D14.

Wotruba, P.R., Benson, R.G. and Schmidt, K.W. (1986): Battle Mountain describes the geology of its Fortitude gold-silver deposit at Copper Canyon. *Mining Engineering* 38, 495-499.

Yun, Suckew and Einaudi, M.T. (1982): Zind-lead skarns of the Yeonhwa-Ulchin District, South Korea. *Econ. Geol.* 77, 1013-1032.